

Target Single Spin Asymmetry in Semi-Inclusive Deep-Inelastic ($e, e'\pi^+$) Reaction on a Transversely Polarized ^3He Target

December 5, 2005

(A new experiment proposal to JLab-PAC29)

B.-Q. Ma, Y.J. Mao, H.X. Ye
School of Physics, Beijing University, P.R. China.

Y. Jiang, H. Lu, Y. Ye
University of Science and Technology of China, Hefei, P.R.China.

J. Yuan, S. Zhou
China Institute of Atomic Energy, Beijing, P.R.China.

W. Chen, D. Dutta, H. Gao (Co-spokesperson), K. Kramer, X. Qian,
Q. Ye, X.F. Zhu, X. Zong
*Duke University and the Triangle Universities Nuclear Laboratory,
Durham, North Carolina*

M. Grosse-Perdekamp, D. Howell, A. Nathan, N. Makins, J.-C. Peng,
L.Y. Zhu
University of Illinois, Urbana-Champaign, Illinois

E. Cisbani (Co-spokesperson), F. Cusanno, S. Frullani, F. Garibaldi,
M.L. Magliozzi, G. Urciuoli, M. Iodice, R. De Leo, L. Lagamba,
S. Marrone, E. Nappi
INFN Roma-I, INFN Roma-III, INFN Bari and University of Bari, Italy

J.-P. Chen, E. Chudakov, R. Feuerbach, J. LeRose, R. Michaels,
S. Nanda, A. Saha, B. Wojtsekhowski
Jefferson Lab, Newport News, Virginia

K. Allada, C. Dutta, A. Kolarkar, W. Korsch
University of Kentucky, Lexington, Kentucky.

R. Gilman, C. Glashauser, X. Jiang (Co-spokesperson/Contact)¹,
E. Kuchina, G. Kumbartzki, R. Ransome.
Rutgers University, Piscataway, New Jersey

F. Butaru, Z.-E. Meziani, B. Sawatzky, P. Solvignon, H. Yao
Temple University, Philadelphia, Pennsylvania

L. Gamberg
Pennsylvania State University at Berks, Reading, Pennsylvania.

T. Averett, T. Holmstrom, A. Kelleher, V. Sulkosky
College of William and Mary, Williamsburg, Virginia.

¹Contact person, email: jiang@jlab.org

Abstract

We propose to carry out a measurement of target Single Spin Asymmetry (SSA) from semi-inclusive electroproduction of positive pions on a transversely polarized ^3He target in Deep-Inelastic-Scattering kinematics. Such SSA will allow for an extraction of the much desired information on the Collins and Sivers asymmetry from the “neutron” in order to probe the quark transversity distributions and the T-Odd Sivers functions. If the Sivers moment $A_{UT}^{n\pi^+}$ turns out to be large and negative in this experiment, as expected from the HERMES data, this will lead to a large d -quark Sivers function opposite to that of u -quark indicating that it carries a large angular momentum opposite to the nucleon spin. If the Sivers moment $A_{UT}^{n\pi^+}$ turn out to be positive, a significant inconsistency will pose a strong challenge to the existing theoretical framework for the Sivers effect. In addition, a combined analysis of E03-004 and this experiment together with the HERMES proton data will provide the first flavor decomposition of both Collins and Sivers effects. We propose to carry out this coincidence experiment in Hall A with the BigBite Spectrometer as the electron-arm and the left HRS spectrometer as the hadron-arm in a setup similar to the E03-004 experiment. The SSA from semi-inclusive ($e, e'K^+$) process will be obtained simultaneously as by-products. We request a total number of 24 days of beam time at an incident beam energy of 6 GeV.

Contents

1	Introduction	6
2	Physics motivation	7
2.1	Transverse target spin related SIDIS cross sections	7
2.2	Transverse target single-spin asymmetry	9
2.3	The HERMES and COMPASS Results	9
2.4	The proposed experiment at JLab in Hall A	13
3	The Proposed Measurement	14
3.1	Overview	14
3.2	The choice of kinematics	16
3.3	Phase space, Collins angle and Sivers angle coverage	16
3.4	The experimental observable	21
3.5	The electron arm: BigBite	21
3.5.1	Single particle background, BigBite single arm trigger and track reconstruction	23
3.6	The hadron arm HRS _L and hadron PID	25
3.6.1	The left-arm RICH detector	25
3.6.2	An option of a pressurized gas Cherenkov vs. RICH	26
3.7	Trigger and offline event selection	27
3.8	Luminosity monitors	28
3.9	The polarized ³ He target	29
3.9.1	Effects of BigBite magnetic field	31
4	Event Rate Estimate and Statistical Uncertainties	31
4.1	Cross section and rate estimate	31
4.2	Cross sections, rates and total number of ($e, e'\pi^+$) events	33
4.3	Statistical uncertainties of Collins and Sivers moments	34
4.4	Systematic uncertainties	34
4.4.1	Effective nucleon polarization in ³ He	35
4.4.2	Corrections to A_{UT} due to target polarization drifts	35
4.4.3	Pions from exclusive ρ production	36
4.4.4	Other terms in SSA and cross sections	36
5	Beam time request, hardware costs and installation time needed	37
5.1	Beam time request	37
5.2	Hardware costs and installation time needed	37
6	Expected Results	38
6.1	Neutron asymmetry $A_{UT}^{n\pi^+}$, Collins and Sivers moments	38
6.2	SSA in SIDIS electroproduction of Kaons	40
7	Relation with other experiments	41

8	Summary	43
9	Acknowledgments	43
A	Appendix-I. Simulation of BigBite background rates and comparisons with test runs	44
B	Appendix-II. Separation of Collins and Sivers asymmetries	46

1 Introduction

The unpolarized parton distribution functions (PDF) have been extracted with excellent precision over a large range of x from DIS, Drell-Yan and other processes after several decades of experimental and theoretical efforts. The comparison of the structure functions in a large Q^2 range with QCD evolution equations has provided one of the best tests of QCD. Motivated by the original “spin crisis” from the European Muon Collaboration experiment in the 1980s, the longitudinal polarized parton distribution functions have been determined with significantly improved precision over a large region of x and Q^2 from polarized DIS experiments carried out at CERN, SLAC, DESY in the last two decades, and most recently at JLab and at RHIC from polarized proton-proton scattering.

What remains elusive is the third class of parton structure functions, the so-called transversity functions, which are chirally odd quark distribution functions. They were discussed for the first time in 1979 by Ralston and Soper [1] and later by Jaffe and Ji in early 1990s [2]. At leading twist if we integrate over the transverse momenta of quarks, there are three quark distribution functions: the unpolarized parton distribution f_1 , the polarized parton distribution g_1 , and the quark transversity distribution, h_1 . These three quark distributions describe the internal dynamics of the hadrons. In the quark-parton models, the nucleon transversity distribution, $h_1(x, Q^2)$ [2] describes the net quark transverse polarization in a transversely polarized nucleon. In the non-relativistic limit, the transversity distribution function is the same as the longitudinal quark polarization distribution function, $g_1(x, Q^2)$. However, one can hardly treat quarks inside nucleon as non-relativistic particles. Therefore, the transversity distribution functions probe the relativistic nature of the quarks inside the nucleon. There are several interesting features about quark transversity distributions. First, they do not mix with gluons, therefore follow simpler evolution and have valence-like behavior [3]. Second, there also exists the Soffer’s inequality [4], $|h_1^q| \leq \frac{1}{2}(f_1^q + g_1^q)$, for the transversity based on the positivity of helicity amplitudes. Lastly, the lowest moment of h_1^q measures a simple local operator, known as the “tensor charge”, which is analogous to the axial charge, and can be calculated from lattice QCD.

Experimental determination of the transversity function is challenging and is not accessible in polarized inclusive DIS measurements because of its chiral-odd nature. To probe the quark transversity functions, an additional chiral-odd object is needed, for example, in double polarized Drell-Yan processes, single target spin azimuthal asymmetries from semi-inclusive deep-inelastic scattering (SIDIS), double spin asymmetries in Λ production from e-p and p-p reactions and single-spin asymmetries in two-hadron production from e-p scattering. It has been proposed that target single spin asymmetry can arise from the following three mechanisms: the so-called Collins asymmetry, the Sivers asymmetry and the Boer-Mulders asymmetry in SIDIS. The quark transversity function in combination with the chiral-odd Collins fragmentation function [5] gives rise to an azimuthal (Collins) asymmetry in $\sin(\phi_h + \phi_S)$, where azimuthal angles of both the hadron (pion) (ϕ_h) and the target spin (ϕ_S) axis are about the virtual photon axis and relative to the lepton scattering plane. The Sivers asymmetry [6, 7, 8] refers to the azimuthal asymmetry of $\sin(\phi_h - \phi_S)$ due to the correlation between the nucleon’s transverse spin and the quark’s transverse momentum, which involves quark orbital motion [9, 10]. The Boer-

Mulders asymmetry [11] is similar to Sivvers asymmetry except the polarization is due to the transversely polarized quarks inside an unpolarized nucleon, which has an azimuthal angular dependence in $\sin(3\phi_h - \phi_S)$. One can disentangle these effects from angular variations of SSA as has been done recently by the HERMES [12] and the COMPASS [13] Collaboration.

The first single target spin azimuthal asymmetry [14] from semi-inclusive DIS pion electroproduction was reported by the HERMES collaboration from a longitudinally polarized proton target. Theoretical interpretations [15, 16, 17, 18, 19, 20] of these data involve transversity-related distributions. Theoretical calculations [21, 22] also suggest that the Collins function has a substantial magnitude despite the fact that the effects of pion and gluon re-scattering tend to cancel. On the other hand, a completely different mechanism which does not involve quark transversity can give rise to SSA as pointed out first by Brodsky, Hwang and Schmidt [23], by Ji and Yuan [24], and by Collins [25]. These authors [23, 24, 25] show that final state interactions from gluon exchange between the outgoing quark and the target spectator system can lead to SSA in SIDIS process.

The recent HERMES SIDIS data on π^- [12] from a transversely polarized proton target seem to require large unfavored Collins functions. Recent studies of the SSA from the $pp \rightarrow \pi X$ process show that the Collins asymmetry is suppressed [26] or at best could only explain [27] the existing data qualitatively. The HERMES data [12] also show for the first time that the Sivvers asymmetry to be positive in the case of π^+ . Single target spin asymmetry (SSA) from SIDIS pion electroproduction from a transversely polarized target has proven to be promising by the recent HERMES [12] and the COMPASS [13] measurements in helping constrain the quark transversity distribution. It will be more so in the near future when new information on currently poorly known Collins fragmentation function becomes available from Belle [28] by analyzing the e^+e^- annihilation data. Therefore, we propose a first SSA measurement in SIDIS electroproduction of positive pions in Hall A from a transversely polarized ^3He target (effective polarized neutron target).

The rest of the proposal is organized as the following. Section II contains the physics motivation for the proposed experiment followed by a discussion on the proposed experiment. Section IV describes the event rate estimate and the statistical uncertainties of the proposed SSA measurement, and Section V contains beam time request, hardware costs and the installation time estimate. The expected results are shown in Section VI, the discussion about their relations to other experiments is contained in Section VII, and lastly the summary. Although most of the technical and physics details in this proposal are identical to the E03-004 experiment, for completeness, we include all the technical details in this document.

2 Physics motivation

2.1 Transverse target spin related SIDIS cross sections

The differential cross section in a SIDIS ($e, e'h$) reaction, in which the beam is not polarized and the target is transversely polarized, can be expressed as the sum of a target

spin-independent and a target spin-dependent term:

$$\begin{aligned} \frac{d\sigma^h}{dx_B dy dz_h d\phi_h} \equiv d\sigma^h &= d\sigma_{UU} + d\sigma_{UT}, \\ &= d\sigma_{UU} + d\sigma_{UT}^{Collins} + d\sigma_{UT}^{Sivers} + d\sigma_{UT}^{others}. \end{aligned} \quad (1)$$

Each term in Eq. 1 can be expressed as convolutions of parton density and fragmentation functions [29]:

$$d\sigma_{UU} = \frac{4\pi\alpha^2 s}{Q^4} (1-y + \frac{y^2}{2}) \sum_q e_q^2 [f_1^q \otimes D_1^q], \quad (2)$$

$$d\sigma_{UT}^{Collins} = \frac{4\pi\alpha^2 s}{Q^4} |S_T| (1-y) \sin(\phi_h + \phi_S) \sum_q e_q^2 [h_1^q \otimes H_1^{\perp q}], \quad (3)$$

$$d\sigma_{UT}^{Sivers} = \frac{4\pi\alpha^2 s}{Q^4} |S_T| (1-y + \frac{y^2}{2}) \sin(\phi_h - \phi_S) \sum_q e_q^2 [f_{1T}^{\perp q} \otimes D_1^q], \quad (4)$$

$$d\sigma_{UT}^{others} = \frac{4\pi\alpha^2 s}{Q^4} |S_T| (1-y) \frac{P_{h\perp}^2}{6z^2 M_N^2} \sin(3\phi_h - \phi_S) \sum_q e_q^2 [h_{1T}^{\perp q} \otimes H_1^{\perp q}]. \quad (5)$$

The azimuthal angles are defined according to the Trento conventions [30] as shown in Fig. 1.

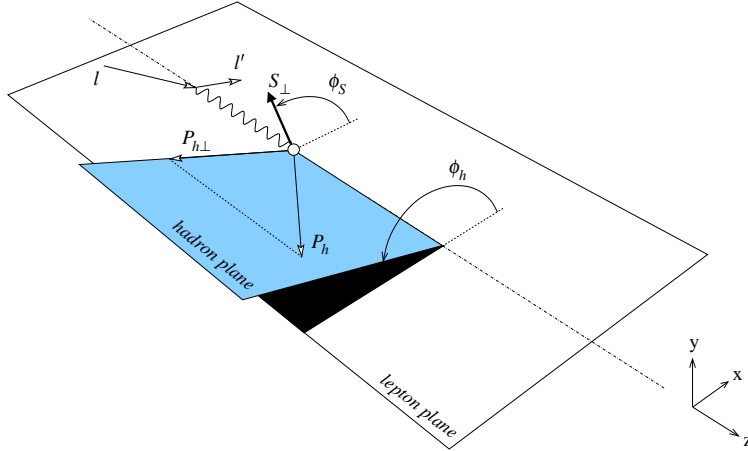


Figure 1: The definition of ϕ_h and ϕ_S according to the Trento conventions.

The convolution in Eq. 2-Eq. 3 represents an integration over transverse momentum of initial (\mathbf{k}_T) and final quark (\mathbf{p}_T) with proper weighting [29], i.e.

$$[.. \otimes ..] = \int d^2 \mathbf{p}_T d^2 \mathbf{k}_T \delta^{(2)}(\mathbf{p}_T - \frac{\mathbf{P}_{h\perp}}{z} - \mathbf{k}_T) [...]. \quad (6)$$

These convolutions can be reduced to simple products if the $|P_{h\perp}|$ -weighted integrations cover to infinite $|P_{h\perp}|$ or explicit \mathbf{p}_T and \mathbf{k}_T dependencies (like Gaussian distributions) are introduced.

2.2 Transverse target single-spin asymmetry

Neglecting the $3\phi_h$ term, which is expected to be small by most model calculations, the target SSA can be defined as:

$$A_{UT} \equiv \frac{1}{|S_T|} \frac{d\sigma_{UT}}{d\sigma_{UU}} \quad (7)$$

The Collins and Sivers asymmetry have different angular dependence:

$$A_{UT}(\phi_h, \phi_S) \equiv \frac{1}{|S_T|} \frac{d\sigma(\phi_h, \phi_S) - d\sigma(\phi_h, \phi_S + \pi)}{d\sigma(\phi_h, \phi_S) + d\sigma(\phi_h, \phi_S + \pi)}, \quad (8)$$

$$= A_{UT}^{Collins} \sin(\phi_h + \phi_S) + A_{UT}^{Sivers} \sin(\phi_h - \phi_S). \quad (9)$$

The HERMES [12] and the COMPASS [13] paper used the notation:

$$A_{UT}^{Collins} \equiv 2\langle \sin(\phi_h + \phi_S) \rangle_{UT} \cdot D_{nn}, \quad (10)$$

$$A_{UT}^{Sivers} \equiv 2\langle \sin(\phi_h - \phi_S) \rangle_{UT} \quad (11)$$

where $D_{nn} \equiv (1-y)/(1-y+\frac{y^2}{2})$ for COMPASS, the HERMES' definition included the longitudinal virtual photon effect $R = \sigma_L/\sigma_T$ to replace D_{nn} with $B(y)/A(x, y)$ where $B(y) = (1-y)$, $A(x, y) = \frac{y^2}{2} + (1-y)\frac{1+R(x, y)}{1+Q^2/\nu^2}$. For this experiment, the differences between D_{nn} and $B(y)/A(x, y)$ are rather small, only at a few percent level.

From Eq. 2-3 we have:

$$A_{UT}^{Collins} \equiv D_{nn} \cdot 2\langle \sin(\phi_h + \phi_S) \rangle_{UT} = D_{nn} \cdot \frac{\sum_q e_q^2 [h_1^q \otimes H_1^{\perp q}]}{\sum_q e_q^2 [f_1^q \otimes D_1^q]}, \quad (12)$$

$$A_{UT}^{Sivers} \equiv 2\langle \sin(\phi_h - \phi_S) \rangle_{UT} = \frac{\sum_q e_q^2 [f_{1T}^{\perp q} \otimes D_1^q]}{\sum_q e_q^2 [f_1^q \otimes D_1^q]}. \quad (13)$$

Although Eq. 12 and Eq. 13 are defined without any ambiguity, in reality however, different experiments usually cover different ranges in the convolution of Eq. 6 due to finite P_{\perp}^h coverages, make it usually impossible for a direct comparison between A_{UT} results from different experiments. Only after explicit \mathbf{p}_T and \mathbf{k}_T dependencies are introduced is such a comparison meaningful. For an ideal experiment with infinite P_{\perp} coverage, SSA asymmetries can be weighted by $|P_{\perp}^h/z_h M_h|$, such that the convolutions in Eq. 6 reduce to products:

$$A_{UT}^{Collins} = \frac{(1-y)}{(1-y+\frac{y^2}{2})} \frac{\sum_q e_q^2 h_1^q(x) \cdot H_1^{\perp(1)q}(z)}{\sum_q e_q^2 f_1^q(x) \cdot D_1^q(z)}, \quad (14)$$

$$A_{UT}^{Sivers} = \frac{\sum_q e_q^2 f_{1T}^{\perp(1)q}(x) \cdot D_1^q(z)}{\sum_q e_q^2 f_1^q(x) \cdot D_1^q(z)}. \quad (15)$$

2.3 The HERMES and COMPASS Results

Recently, the HERMES Collaboration [12] and the COMPASS Collaboration [13] reported results on single-spin asymmetries from a transversely polarized target from semi-inclusive electroproduction of hadrons in DIS kinematics.

The HERMES SSA results [12] were obtained from a transversely polarized proton target from semi-inclusive electroproduction of pions in DIS kinematics. The asymmetries depend on the azimuthal angles of both the pion (ϕ_h) and the target spin (ϕ_S) axis about the virtual photon axis and relative to the lepton scattering plane. Signal due to the unknown Collins fragmentation function in conjunction with the previously unmeasured quark transversity distribution has been seen in the extracted Fourier component of $\langle \sin(\phi_h + \phi_S) \rangle$ from the data as shown in Fig. 2. The data are presented as a function of x (left panel) and z (right panel), respectively for both the positive pions and the negative pions. The Sivers asymmetry due to the correlation between the quark transverse polarization and quark transverse momentum was also extracted for the first time from a transversely polarized proton target from the Fourier component of the azimuthal $\langle \sin(\phi_h - \phi_S) \rangle$ distribution shown in Fig. 2.

The HERMES data show rather larger negative π^- Collins moments. This surprising feature might be explained by the possibility that disfavored fragmentation could be of unexpected importance and may enter with a sign opposite to that of the favored case. The HERMES analysis of single-spin asymmetry from events of exclusive vector meson production from a transversely polarized proton target show that Sivers asymmetry extracted from semi-inclusive charged pion electroproduction might be affected by exclusive vector meson productions. A very interesting observation from the HERMES data is that the Sivers moment extracted from the positively charged pion is positive over the entire x and z range of the experiment, while the Sivers moment from the negatively charged pion seems to be consistent with zero.

By combining the single-spin asymmetries from semi-inclusive pion electroproduction in DIS kinematics both from a transversely polarized proton target [12] and a longitudinally polarized proton target [14], the HERMES collaboration extracted the sub-leading-twist contribution [31] to the longitudinal case. They found that the contribution to the π^+ case to be significantly positive and dominates the longitudinal single target spin azimuthal asymmetry. In the π^- case, the contribution was found to be small.

The COMPASS collaboration reported first measurements [13] of the Collins and Sivers asymmetries of charged hadrons from semi-inclusive scattering of muons from a transversely polarized ${}^6\text{LiD}$ target in the deep-in-elastic kinematic region. Both the Collins asymmetry and the Sivers asymmetry are consistent with zero within experimental uncertainties. One may expect the transversity of u quark and d quark to have opposite sign. Therefore, some cancellation in single-spin asymmetries may exist in measurements using a transversely polarized target, which may explain the smallness of the COMPASS Collins and Sivers asymmetries. Results with improved statistical errors (a factor of two) by including COMPASS 2003 and 2004 data will be released in the near future. COMPASS is also planning on new measurements with a transversely polarized proton target. The COMPASS results are shown in Fig. 3.

There has been significant theoretical efforts in understanding the quark transversity distributions in the last decade or so, perhaps more so in the last few years motivated by the experimental progress, particularly by the HERMES [14, 12] and the COMPASS [13] results. We will not attempt here to discuss all these efforts, but will discuss two recent developments briefly below.

The role of intrinsic quark transverse momentum, \mathbf{k}_\perp in semi-inclusive hadron electro-

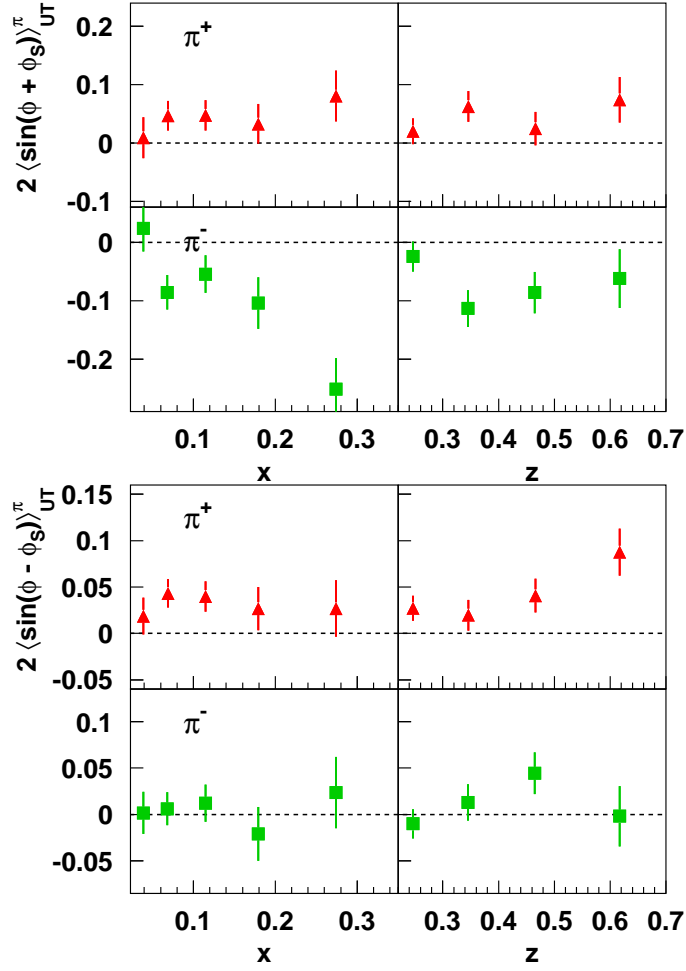


Figure 2: The HERMES results of virtual-photon Collins (Sivers) moments for charged pions as labeled in the upper (lower) panel, as a function of x and z . The data are shown with statistical errors only. For details, see Ref. [12].

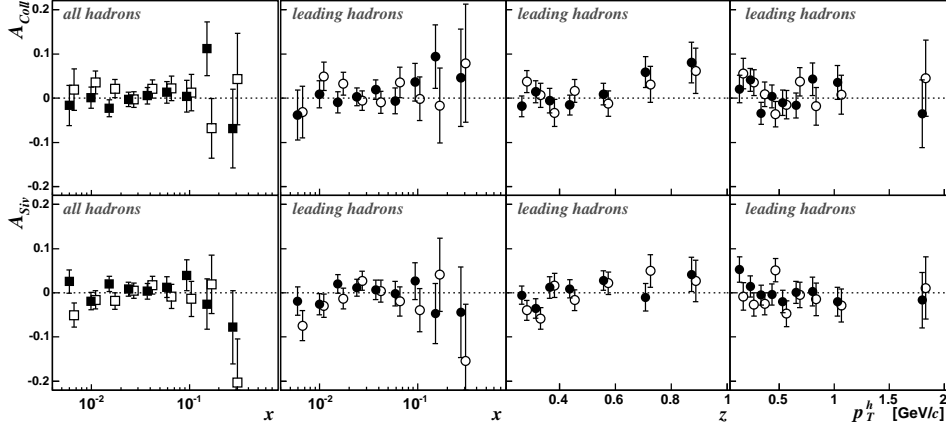


Figure 3: The COMPASS results on the Collins asymmetry (top) and the Sivers asymmetry (bottom) as a function of x , z , and p_T^h for positive hadrons (solid circles) and negative hadrons (open circles) with statistical errors only. The first column is for all hadrons and the other three columns are for leading hadrons only.

production in DIS scattering kinematics has been studied [32] within QCD parton model at leading order. The so-called Cahn effect, referring to the dependence of the unpolarized cross-section to the azimuthal angle between the leptonic and hadronic planes has been compared with data to estimate the average values of \mathbf{k}_\perp both for quark distribution and fragmentation functions. The authors of [32] then apply the resulting picture to describe the HERMES data on the weighted single-spin asymmetries of semi-inclusive pion lepto-production at DIS kinematics, which allows the extraction of simple models for the quark Sivers functions. In a more recent paper by Anselmino *et al.* [33], Sivers function for u and d quark has been extracted by combining the HERMES results from a transversely polarized proton target and the COMPASS results from a transversely polarized deuteron (${}^6\text{LiD}$) target. Predictions for the JLab kinematics for the Sivers asymmetries are given by the authors of [33], as well as single spin asymmetries for Drell-Yan processes at RHIC and GSI.

Recently Vogelsang and Yuan [34] studied single spin (Collins and Sivers) asymmetries from a transverse polarized target in semi-inclusive DIS electroproduction of hadrons using the QCD factorization approach. Simple Collins and Sivers functions were obtained by fitting the HERMES data. These simple Collins and Sivers functions were able to describe the COMPASS results reasonably well. The authors made predictions for various processes in pp collisions based on the fitted parameterization for the Sivers function. Using this approach, Yuan [35] made predictions for single spin asymmetries for semi-inclusive pion electroproduction from a transversely polarized “neutron” (${}^3\text{He}$) target at the JLab kinematics. The Collins asymmetry for neutron is found to be smaller than those from the proton based on the HERMES data and the isospin symmetry. The situation for the Sivers asymmetry is more complicated and asymmetry for π^+ in the case of the neutron can be as large as 40-50%. The main reason for such a large Sivers asymmetry is that a large Sivers function for the d quark in the proton with an opposite sign to that of the u quark in the proton is required in order to fit the HERMES data. Based on the

isospin symmetry, one expects a large Sivers function for the u quark in the neutron and the π^+ production is dominated by the u -quark fragmentation.

2.4 The proposed experiment at JLab in Hall A

Jefferson Lab is in a unique place to make important contribution to the study of the quark transversity distributions, a fundamental and timely subject. The polarized inclusive DIS program at Jefferson has made important, well-recognized contributions already in the field, particularly in the study of the nucleon longitudinal polarization distributions in the large x region. Recently, the Jefferson Lab CLAS collaboration reported [36] the first evidence for a non-zero beam-spin azimuthal asymmetry in the semi-inclusive production of positive pions in the deep inelastic scattering region. Furthermore, the study of the pion multiplicities as a function of x has been carried out and no x dependence has been observed, and this finding is consistent with the assumption of factorization. Whether factorization is valid or not for Jefferson Lab kinematics had been a major concern for all semi-inclusive DIS experiments at Jefferson Lab. The HERMES results [12] show very interesting feature between positive pions and negative pions from a transversely polarized proton target. COMPASS shows Collins and Sivers asymmetries are consistent with zero within experimental errors from a transversely polarized ${}^6\text{LiD}$ target. Single-spin asymmetry measurements from semi-inclusive positive pion electroproduction in DIS kinematics from a transversely polarized ${}^3\text{He}$ target (effective neutron target) is essential for the following reasons.

- The separate determination of the Collins and Sivers asymmetries from a transversely polarized neutron “target” as proposed in this proposal employing a polarized ${}^3\text{He}$ target is very important. While the Collins asymmetries for the neutron are expected to be small based on the HERMES results and isospin symmetry, larger than expected Collins asymmetry in the case of the neutron will seriously challenge the state-of-the-art models of the transversity and the physics associated with these models. The predicted Sivers asymmetries for the π^+ in the case of the neutron can be as large as 40-50%, though the situation is very complicated and predictions vary over a large range.
- The proposed positive pion measurements are complementary to the previously approved negative pion measurements also employing the polarized ${}^3\text{He}$ target in Hall A. We propose the same kinematics as those of the negative pion measurements. Therefore, these two experiments can run back-to-back in an efficient way.
- The combined measurements of π^+ and π^- will allow the study of the surprising feature suggested by the comparison between the HERMES π^+ and π^- results that the fragmentation in the case of the disfavored quark flavor seems to play an important role and may enter with an opposite sign as that of the favored case for the Collins moment. The HERMES experiment was carried out with a transversely polarized proton target. Therefore, measurements of charged pion semi-inclusive electroproduction in the DIS region in an x -range comparable to that of the HERMES from a transversely polarized “neutron” target will be very important.

- The proposed π^+ measurements and the proposed experiment on π^- from Hall A employing a transversely polarized ^3He target (effective polarized neutron target) in combination with the HERMES results [12] from the proton in the similar x region will allow for a flavor separation of quark transversity distributions, especially in the case of the Sivers asymmetries.

3 The Proposed Measurement

3.1 Overview

The experimental configuration for the proposed experiment here will be the exactly same as that of experiment E03-004, the neutron transverse SSA measurement in $n^\uparrow(e, e'\pi^-)$ reaction, except that the magnet polarity of the HRS_L spectrometer will be reversed for the π^+ detection. For completeness, we include all these details here although many sections in this document are identical to the update document of E03-004.

We plan to study the target single spin asymmetry (SSA) in the semi-inclusive deep-inelastic $\vec{n}(e, e'\pi^+)X$ reaction on a transversely polarized ^3He target in Hall A with a 6 GeV beam. The $(e, e'K^+)$ events will be treated as by-products. The average beam current will be $\approx 15 \mu\text{A}$. Although a polarized beam is not required to perform the SSA measurements, we request a 80% polarized electron beam for parasitic double-spin asymmetry measurements. Analysis of SSA will sum over the two beam helicities.

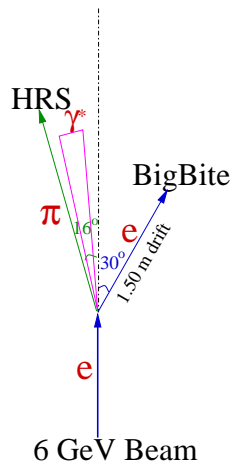


Figure 4: The experimental arrangement, target polarization is in the plane that is perpendicular to the plane of $\vec{q} \wedge (\vec{q} \times \vec{p}_\pi)$.

The experiment will use the Hall A left side high resolution spectrometer (HRS_L) situated at 16° as the hadron arm, and use the BigBite spectrometer at 30° beam-right as the electron arm. The BigBite detector configuration will be exactly the same as in Hall A G_E^n experiment [37] (E02013), which is scheduled to take production data in February, 2006. The drift distance to the BigBite dipole magnet will be 1.50 meter, instead of the 1.10 meter in E02013. Since this experiment is a coincidence experiment with the HRS_L at a relatively low rate, the HRS spectrometer can be used for interaction

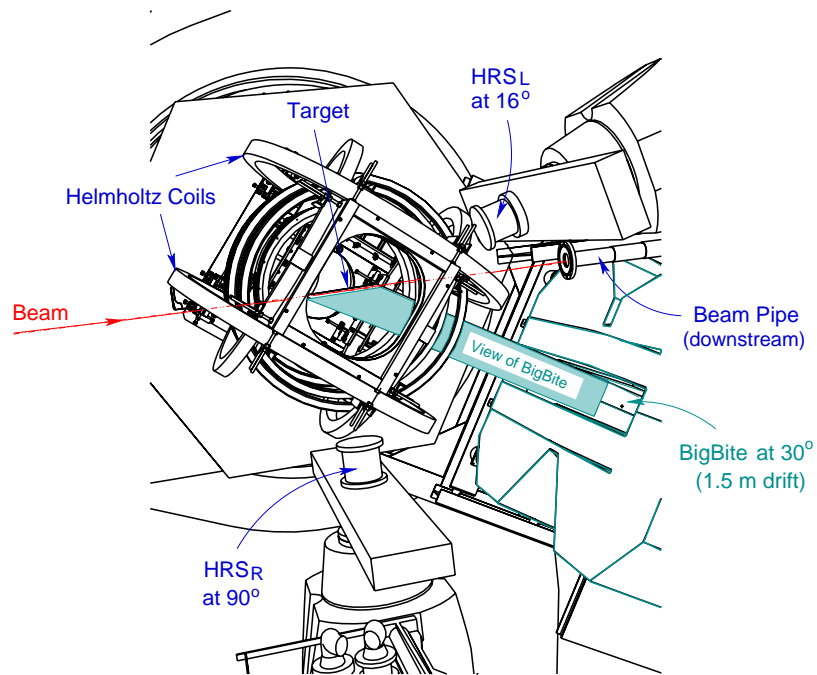


Figure 5: A top view near the pivot. The left HRS is shown at 16° , the BigBite dipole magnet is shown at 30° beam right and at a drift distance of 1.5 meters. The right HRS is at 90° as a luminosity monitor. The target coils are arranged to avoid interference with the beam line and the spectrometers.

vertex reconstruction such that most of the complications associated with the BigBite wire chamber track reconstruction can be eliminated, in contrast to the case of the G_{En} experiment. In addition, when a tight coincidence timing cut is further required we expect that the majority of the background tracks and random hits in the BigBite wire chambers can be easily eliminated.

The Hall A high density polarized ^3He target will be used with a 40 cm long cell. The Helmholtz coils and laser optics need to be modified to provide a target polarization along two specific orientations: the vertical direction and the transverse in-plane relative to the beam direction. The experimental arrangement is illustrated in Fig. 4 and a close-up view near the pivot is shown in Fig. 5.

3.2 The choice of kinematics

The definitions of the kinematics variables are the following: Bjorken- x , which indicates the fractional momentum carried by the struck quark, $x = Q^2/(2\nu M_N)$, M_N is the nucleon mass. The momentum of the outgoing hadron is p_h and the fraction of the virtual photon energy carried by the hadron is: $z = E_h/\nu$. W is the invariant mass of the whole hadronic system and W' is the invariant mass of the hadronic system without the detected hadron. We have:

$$\begin{aligned} W^2 &= M_N^2 + Q^2\left(\frac{1}{x} - 1\right), \\ W'^2 &= (M_N + \nu - E_\pi)^2 - |\vec{q} - \vec{p}_\pi|^2. \end{aligned} \tag{16}$$

We chose to cover the highest possible W with a 6 GeV beam, $2.33 < W < 3.05$ GeV, corresponding to $0.135 < x < 0.405$ and $1.31 < Q^2 < 3.10$ (GeV/c) 2 . We also chose to detect the leading fragmentation pion which carries $z \approx 0.5$ of the energy transfer to favor the current fragmentation. The value of W' is also chosen to be as high as possible with a cut of $W' > 1.5$ GeV to avoid contributions from resonance production channels. The kinematics for each x -bin center are listed in Table 4.3. Because of the large momentum acceptance of the BigBite spectrometer, only one BigBite momentum setting is needed to cover all the kinematics listed in Table 4.3. A hadron arm momentum setting of $p_\pi = 2.4$ GeV/c is chosen for the entire experiment. The corresponding values of W' and z are listed in Table 4.3.

3.3 Phase space, Collins angle and Sivers angle coverage

The phase space coverage is obtained from a detailed Monte Carlo simulation which includes realistic spectrometer models as well as target and detector geometry. The coverage in the (Q^2, x) and (W, x) planes is shown in Fig. 6, and the coverage in the (W', x) and (P_\perp, x) planes is shown in Fig. 7, color coded for each x -bin.

The angular coverage of ϕ_h^l and ϕ_S^l is shown in Fig. 8 and Fig. 9. Two settings of target spin orientation will be employed to form target SSA at each setting with $\langle\phi_S^l\rangle = 0^\circ, 90^\circ, 180^\circ$ and 270° , respectively. The Collins angle coverage is shown in Fig. 10. For every x -bin in this experiment, the full 2π range of the Collins angle is covered. The Sivers angle coverage is shown in Fig. 11.

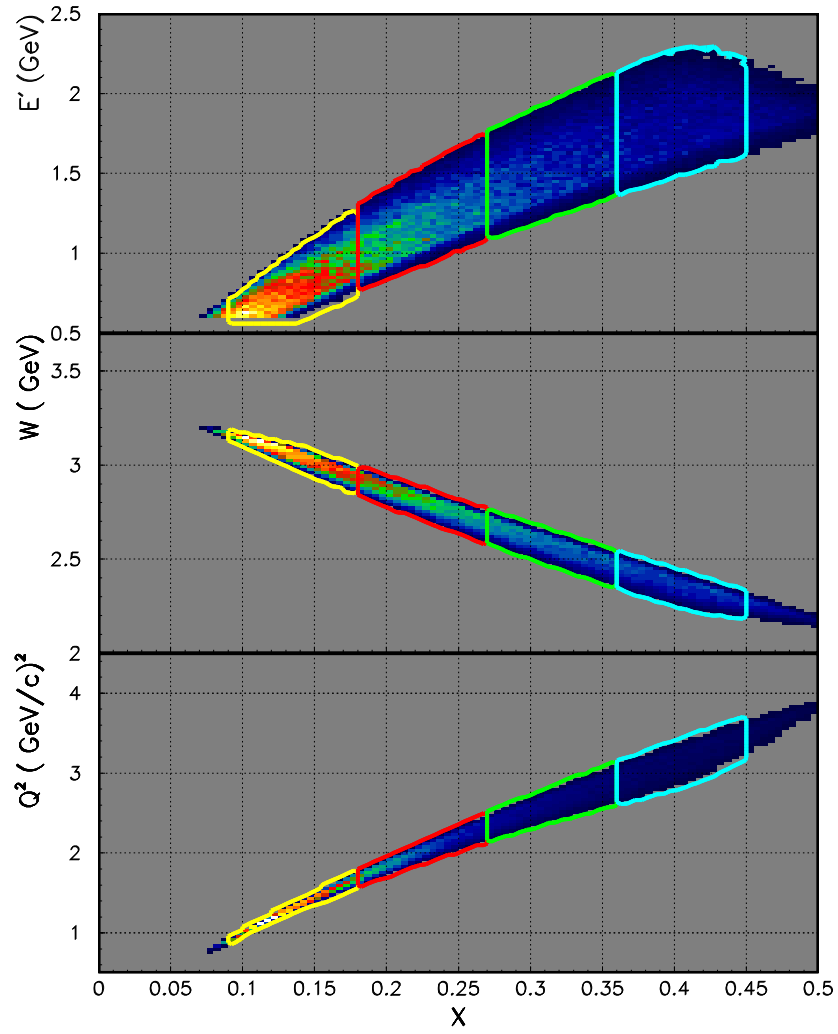


Figure 6: The available phase space in the (Q^2, x) and (W, x) planes with each x -bin shown in different colors.

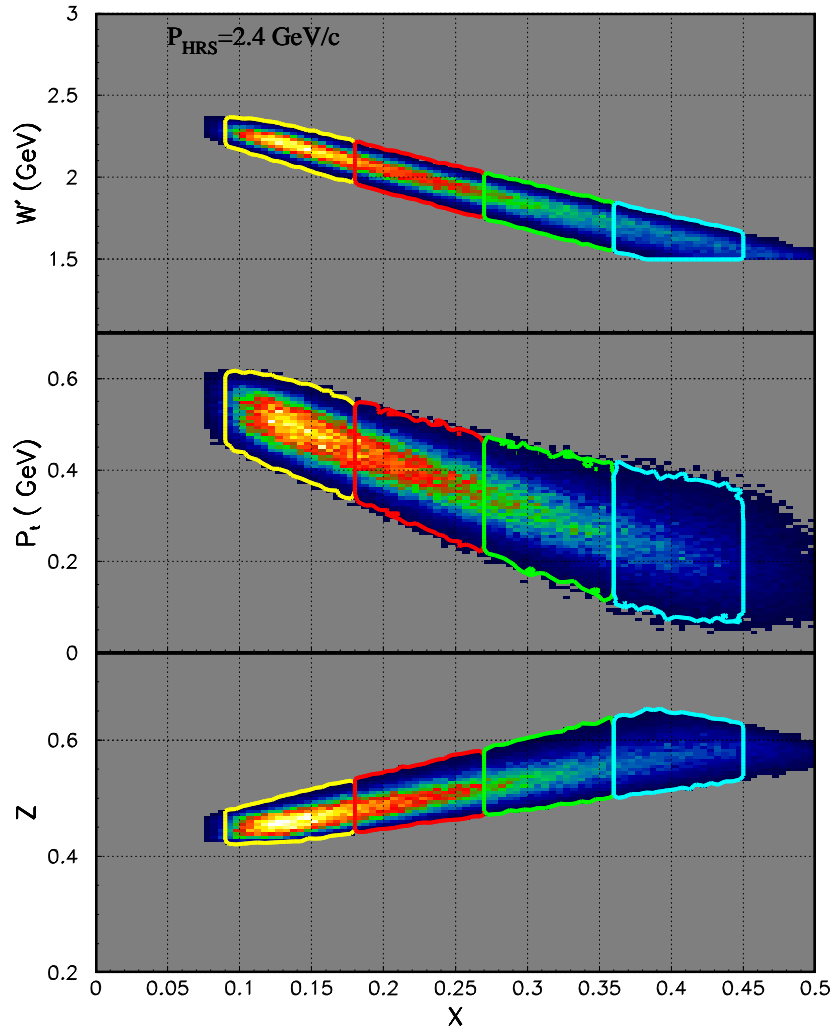


Figure 7: The same as in Fig. 6, phase space coverage in (W', x) , (P_{\perp}, x) and (z_{π}, x)

Table 1: Nominal kinematics of each x -bin (central value) for beam energy of $E = 6.0$ GeV. One BigBite setting will cover all the kinematics listed. E' and θ_e are the electron arm momentum and angle. θ_q indicates the direction of \vec{q} . The hadron arm angle is fixed at 16° .

E' GeV	θ_e deg.	$\langle x \rangle$	W GeV	Q^2 GeV ²	θ_q deg.	z_π	p_π GeV/c	W' GeV
$\theta_\pi = 16.0^\circ$								
0.815	30.0	0.135	3.050	1.310	4.40	0.46	2.40	2.20
1.246	30.0	0.225	2.793	2.003	7.22	0.51	2.40	1.99
1.612	30.0	0.315	2.554	2.592	9.93	0.55	2.40	1.80
1.925	30.0	0.405	2.331	3.095	12.52	0.59	2.40	1.62

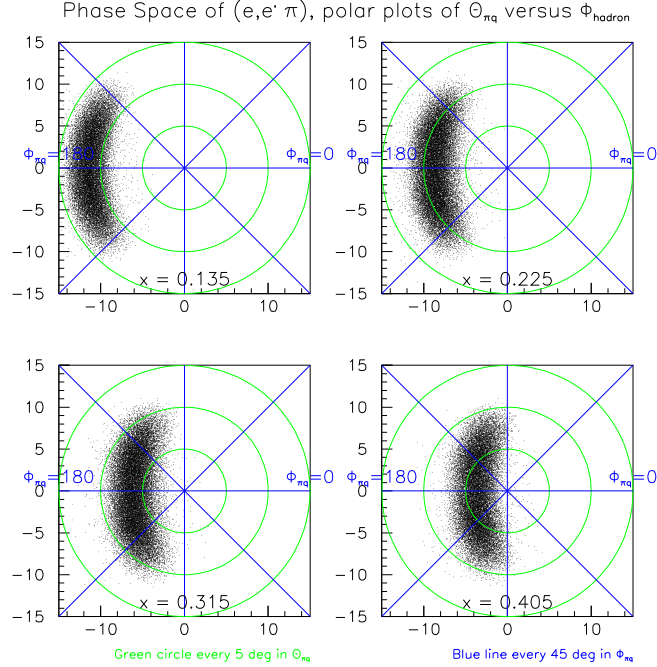


Figure 8: The angular coverage of ϕ_h^l is shown for each x -bin, viewed along \vec{q} .

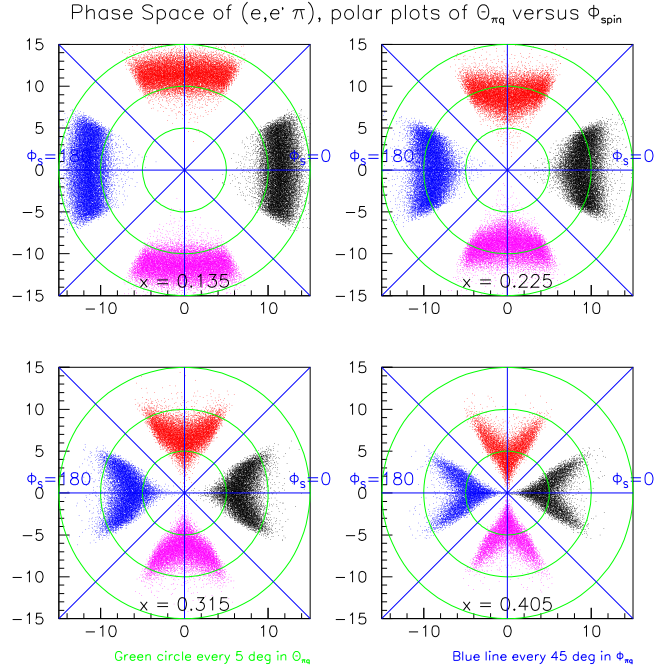


Figure 9: The angular coverage of ϕ_S^l is shown for each x -bin, viewed along beam. Black: $\phi_S^l = 0^\circ$. red: $\phi_S^l = 90^\circ$, blue: $\phi_S^l = 180^\circ$, purple: $\phi_S^l = 270^\circ$.

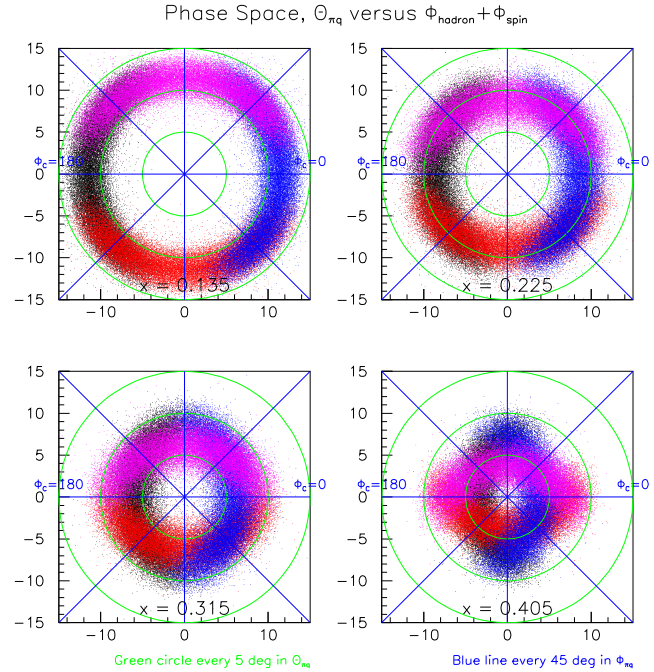


Figure 10: The Collins angular coverage of $\phi_{Collins} = \phi_h^l + \phi_S^l$ is shown for each x -bin. Black: $\phi_S^l = 0^\circ$. red: $\phi_S^l = 90^\circ$, blue: $\phi_S^l = 180^\circ$, purple: $\phi_S^l = 270^\circ$. For every x -bin in this experiment, the full 2π range of the Collins angle is covered.

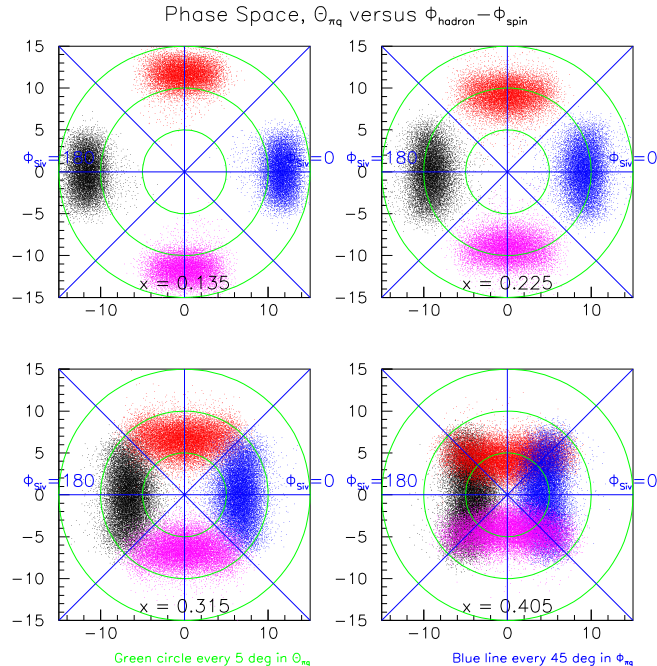


Figure 11: The Siverson angular coverage of $\phi_{Siverson} = \phi_h^l - \phi_S^l$ is shown for each x -bin. Black: $\phi_S^l = 0^\circ$. red: $\phi_S^l = 90^\circ$, blue: $\phi_S^l = 180^\circ$, purple: $\phi_S^l = 270^\circ$.

3.4 The experimental observable

The target single spin asymmetry $A_{UT}^h(\phi_h, \phi_S)$ can be obtained directly from the luminosity-normalized yield:

$$A_{UT}^h(\phi_h, \phi_S) = \frac{1}{P_T} \cdot \frac{N(\phi_h, \phi_S) - N(\phi_h, \phi_S + \pi)}{N(\phi_h, \phi_S) + N(\phi_h, \phi_S + \pi)} \quad (17)$$

The relative luminosity will be monitored by various spectrometer singles rates and the downstream luminosity monitors. In addition, frequent target spin-flips, once every 15-30 minutes, are expected to further reduce the uncertainties in the luminosity ratio.

3.5 The electron arm: BigBite

The BigBite spectrometer will be located at 30° and at a drift distance of 1.50 m, instead of the 1.1 m drift in E02013. The BigBite detector package will be identical to what will be used in the G_E^n experiment (E02013). Three sets of wire chambers will be used to provide tracking information followed by a pre-shower, scintillator and shower assembly to provide trigger and particle ID for the electrons. The BigBite dipole magnet will be set at the full current with $|\vec{B}| = 1.2$ T. Charged particles originated from the target with momentum less than 0.2 GeV/c will not reach the detectors, as shown in Fig. 12.

The BigBite collaboration has already built three sets of wire chambers, each with U-U', V-V' and X-X' planes. The sense wire separation is 2.0 cm, corresponding to a drift cell size of 1.0 cm and a maximum drift time of 100 ns. A GEANT-3 Monte Carlo

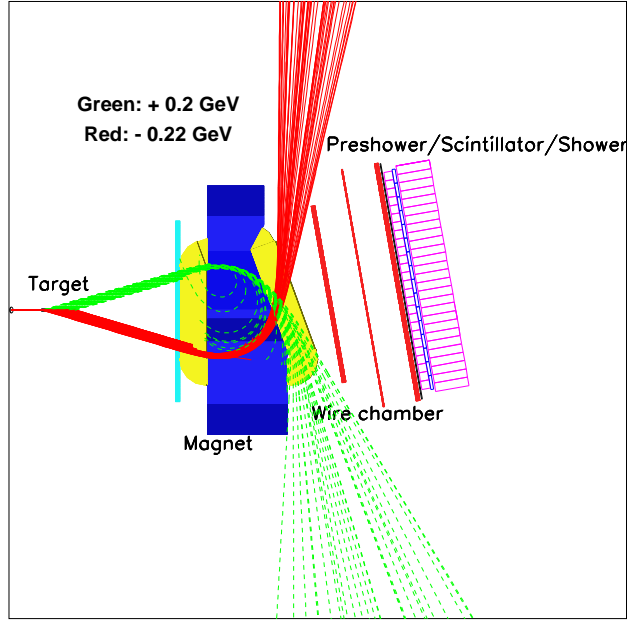


Figure 12: Charged particle trajectories through the BigBite magnet. Positive particles with momentum less than 200 MeV/c and negative particles with momentum less than 220 MeV/c will not reach the detectors. The location of wire chambers, pre-shower, trigger scintillator planes and shower lead glass arrays are also indicated.

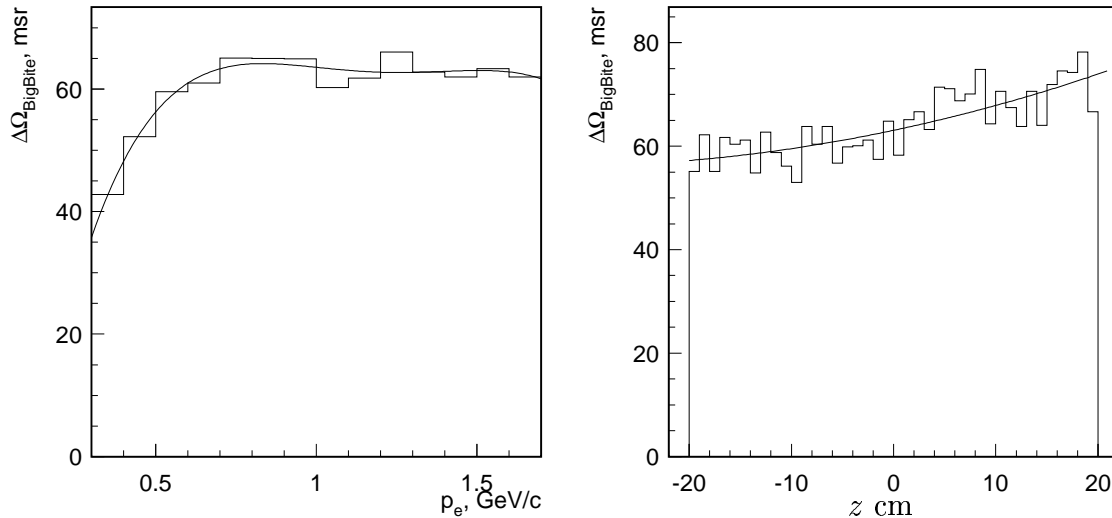


Figure 13: BigBite acceptance as a function of particle momentum (left) and as a function of interaction point (right).

simulation [37] has shown that with a typical chamber resolution of $200\ \mu\text{m}$, the momentum resolution ($\delta p/p$) is $\approx 2\%$. The angular resolution is $3.0\ \text{mrad}$ in each direction, causing a few MeV uncertainty in P_{\perp} reconstruction. The vertex resolution (at 30°) will be better than $2.0\ \text{cm}$ along the beam. Since this experiment does not seek to resolve any structure in the final states, and the SIDIS events will be grouped in rather large x -bins, the momentum and angular resolutions designed for E02-013 will be adequate for this experiment.

The electron particle identification (PID) will be provided by a set of pre-shower and shower detectors. The pre-shower blocks are made of TF-5 lead glass, $10 \times 10 \times 37\ \text{cm}^3$ each, covering an active area of $210 \times 74\ \text{cm}^2$, with $10\ \text{cm}$ (3 r.l.) along the particle's direction. The total absorption shower blocks are made of TF-2 lead glass, $8.5 \times 8.5 \times 34\ \text{cm}^3$ each, covering an active area of $221 \times 85\ \text{cm}^2$, with $34\ \text{cm}$ (13 r.l.) along the particle's direction. The total depth of lead glass is enough to contain electron showers with energies up to $10\ \text{GeV}$, with an energy resolution of $8.0\%/\sqrt{E}$. A typical pion rejection factor of 100:1 is expected from offline cuts that combines pre-shower and shower information. Based on Hall C SOS spectrometer data taken at a similar kinematics, the expected worst case singles π^-/e^- ratio in BigBite will be no more than 100:1 for this experiment. Since we are only interested in coincidence events in this experiment, a cut of coincidence TOF and a cut of two-particle vertex consistency will reduce the random π^- contamination to a negligible level (see Table 5).

The BigBite acceptance as a function of particle momentum and interaction point is shown in Fig. 13. An average solid angle of $64\ \text{msr}$ is expected, with the vertical angle $\Delta\theta_t = \pm 240\ \text{mrad}$ ($\pm 13.7^{\circ}$) and the horizontal angle $\Delta\phi_t = \pm 67\ \text{mrad}$ ($\pm 3.8^{\circ}$).

3.5.1 Single particle background, BigBite single arm trigger and track reconstruction

The background rates in the BigBite detectors are calculated using the Monte Carlo simulation code GDINR [38]. For particles with momentum above $200\ \text{MeV}/c$, the integrated electron rate is less than $65\ \text{kHz}$, π^- rate is $380\ \text{kHz}$, π^+ rate is $500\ \text{kHz}$ and the positron rate is $20\ \text{kHz}$. The majority of the charged particle background comes from low energy protons with $p > 200\ \text{MeV}/c$ ($T_p > 21\ \text{MeV}$) at a rate of $2.0\ \text{MHz}$, comparable to the situation of E02-013. The majority of these protons will be stopped by the pre-shower detector and never reach the trigger scintillators. The BigBite single-arm trigger will be formed from a logical AND of a scintillator hit and an energy deposition of at least $200\ \text{MeV}$ in the pre-shower or in the shower detectors. Only a small fraction of charged pions are expected to deposit enough energy in pre-shower and shower to generate such a trigger. The raw BigBite single-arm trigger rate is expected to be less than $200\ \text{kHz}$.

The low energy particle background on BigBite wire chambers is the major concern of this experiment. An extensive Monte Carlo background simulation has been carried out, and has been cross checked with rate information from several test runs. More details of the simulation are attached in Appendix-I. According to the simulation, the wire chamber rate will be at the level of $10\text{-}20\ \text{MHz}$ per chamber, similar to the situation in the G_E^n experiment (E02-013). Recently, drift chambers of a similar design have performed well during the Hall C hyper-nuclear experiment at a comparable background rate.

By taking the BigBite magnet to a 1.5 meter drift distance, extra space is available before the magnet and between the detectors and the downstream beam pipe to construct shielding and to install collimators. A steal plate of 2 inch thickness on the downstream side, for example, can reduce the wire chamber activity by a factor of ten. The effectiveness of side shielding is illustrated in a GEANT simulation as shown in Fig. 14. We expect that by the time G_E^n (E02-013) starts taking production data in February 2006, shielding improvements of BigBite will make the background level acceptable to both the G_E^n experiment and this experiment.

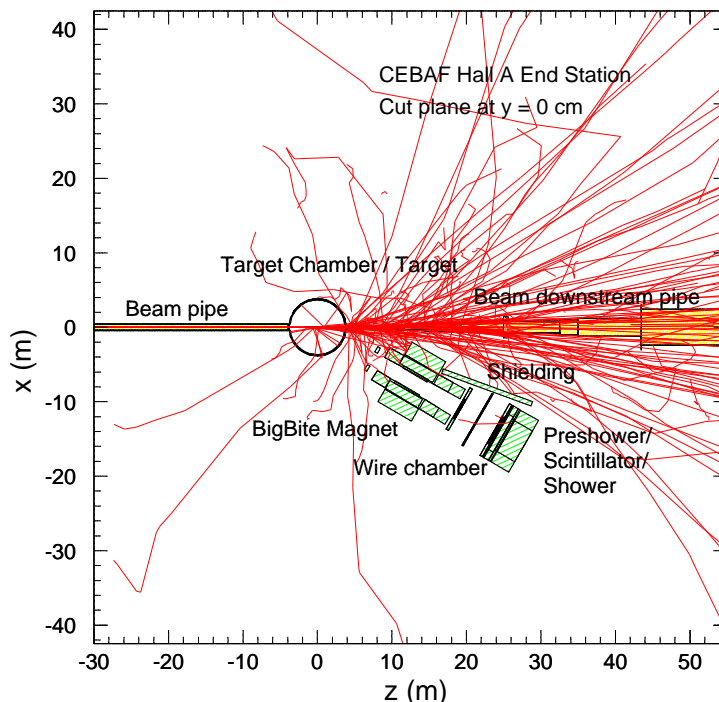


Figure 14: An illustration of the BigBite detector shielding plan. Most of the low-energy background particles can be shielded from hitting the wire chambers by a 2 inch steal plates on the downstream side.

Since the drift time window is 100 ns, the average multiplicity will be $1 \sim 2$ hits/plane for each trigger. This type of chamber background activity could result in several candidate tracks for a single arm experiment, or for an $(e, e'n)$ type measurement, such as in E02-013. For two-charge particle coincidence measurement, such as this experiment, in which the trigger involves the timing coincidence from two spectrometers, the on-line trigger will be rather clean, especially when the HRS_L singles trigger has a relatively low rate. In addition, high resolution vertex information from HRS_L on a long target helps in reducing the offline tracking ambiguity in BigBite, especially when the reconstruction on the HRS_L side is very clean. For BigBite tracking, the correct hit on the third chamber will be chosen closest to the center of the maximum shower in lead glass blocks. Since the BigBite dipole magnet does not cause much bending in the transverse direction, a straight line between the HRS_L reconstructed vertex and the center of the maximum shower at the

Table 2: Single arm rates in HRS_L.

p (GeV/c)	Rate in HRS _L (Hz)			
	π^+	K^+	p	e^+
2.40	1687	342	962	0.2

calorimeter serves as the starting point of track reconstruction. In the dispersive direction, the location of the maximum shower cluster helps in track selection. Furthermore, the reconstructed particle momentum has to be consistent with the energy deposited in the calorimeter.

The G_E^n collaboration is planning an extensive optics calibration data taking during the BigBite commissioning in February, 2006. This set of optics data will also be used for the transversity experiment, after corrections in alignments and in differences of drift distance. Data taken during the E02-013 experiment will help to improve our BigBite magnet model, such that the acceptance will be well-understood, to better than $\pm 5\%$ level in the central region of the BigBite spectrometer. Although this experiment is designed to measure target spin correlated asymmetries, we expect that reasonable accuracies can also be reached for cross section ratios ($\pm 3\%$), spin-dependent and spin-independent multiplicities ($\pm 3\%$) and absolute cross sections ($\pm 5-8\%$).

3.6 The hadron arm HRS_L and hadron PID

The Hall A left-arm high resolution spectrometer (HRS_L) has been used in many experiments which requires good particle identifications and accurate knowledge of the acceptance ($\pm 3\%$). Absolute cross sections from polarized ^3He targets have been measured to a $\pm 5\%$ level in experiment E94-010 at a similar spectrometer angle.

This experiment will use a HRS_L detector package similar to the configurations in the Penta-quark search and in the Hyper-nuclear experiments. The π^+/K^+ separation will be achieved by two independent ways: (i) a set of two threshold aerogel Cherenkov counters; (ii) a ring imaging Cherenkov detector (RICH). A third independent separation based on differences in coincidence time-of-flight can serve as a cross check.. At a momentum of 2.4 GeV/c, charged pions will trigger both aerogel Cherenkov A1 ($n=1.015$) and A2 ($n=1.055$) while charged Kaons will only trigger A2.

The expected HRS_L singles rates are listed in Table. 2. The single-arm HRS_L trigger rate will be about 3.0 kHz, dominated by π^+ . Through the path of 25 meters in HRS_L, the time-of-flight for different charge particles at $p = 2.4$ GeV/c are listed in Table 3. Assuming a TOF resolution of $\sigma = 0.85$ ns, protons will be rejected with 7.2σ by flight time alone. The π^+/K^+ TOF separation will be at 2.05σ .

3.6.1 The left-arm RICH detector

The left-arm RICH detector [39] was designed to optimally identify 2 GeV kaon from pion (and proton). The detector consists of a Freon (C_6F_{14}) radiator with a refractive index $n = 1.28$ followed by a proximity gap of 10 cm and a multi-wire/pad proportional

Table 3: TOF and Δ_{TOF} (relative to light-speed e^\pm) for the relevant kinematics, and number of sigma (assuming a coincidence TOF resolution of 850 ps)

	HRS $p = 2.40$ GeV/c			
	e^\pm	π	K	p
TOF (ns)	83.39	83.53	85.14	89.54
Δ_{TOF}	0.00	0.14	1.75	6.15
N_σ		0.17	2.05	7.23

Table 4: The performance of the RICH for the present configuration and the configuration after the upgrade.

RICH Configuration	Momentum [GeV/c]	σ_{θ_π} [mr]	$\theta_\pi - \theta_K$ [σ_{θ_π}]	π Rejection at 95% efficiency
Existing	2	5	6	> 1000
Existing	2.4	4.8	4	120
Upgraded:				
C ₅ F ₁₂ Gap = 15.5 cm	2.4	4.2	5.7	> 1000

chamber. The 11520 pads are read out by a multiplexed Sample&Hold electronics, with a VME based ADCs. The RICH has operated successfully in 2004 and 2005 for the hyper-nuclear experiment E94-107, providing a Cherenkov angular resolution of 5 mrad ($\theta_\pi - \theta_K = 6\sigma_{\theta_\pi}$) corresponding to a pion rejection factor greater than 1000 at 95% efficiency (see table 4).

At a momentum of 2.4 GeV/c, the RICH will be able to separate π^+/K^+ to $4.0 \sigma_{\theta_\pi}$ with a pion rejection factor of 120, suitable for the requirement of this experiment.. However, minor upgrades of the present RICH can be made at a modest cost to improve the separation to $5.7 \sigma_{\theta_\pi}$ corresponding to a pion rejection factor of 1000. These improvements include adding a stainless steel frame spacer to increase the proximity gap to 15.5 cm, and replacing the present radiator with a different kind of freon (C₅F₁₂ n=1.24). The cost of these upgrade is estimated to be at \$15-20k. INFN-ROME group will take on the technical responsibility of the RICH upgrade.

A GEANT3 based Monte Carlo has been developed to investigate the performance of the upgraded RICH. The results are summarized in Table 4 and are shown in Fig. 15 for the present and the upgraded RICH.

3.6.2 An option of a pressurized gas Cherenkov vs. RICH

The Hall A Penta-quark experiment [40] is investigating the option of a pressurized gas Cherenkov in HRS_L. This option calls for a pressurized C₄F₁₀ gas at about 1.6 Atm ($n = 1.0025$). Charged pions at 2.4 GeV/c will produce on average 12 photo-electrons while charged kaons are below the threshold. A combination of the pressurized gas Cherenkov

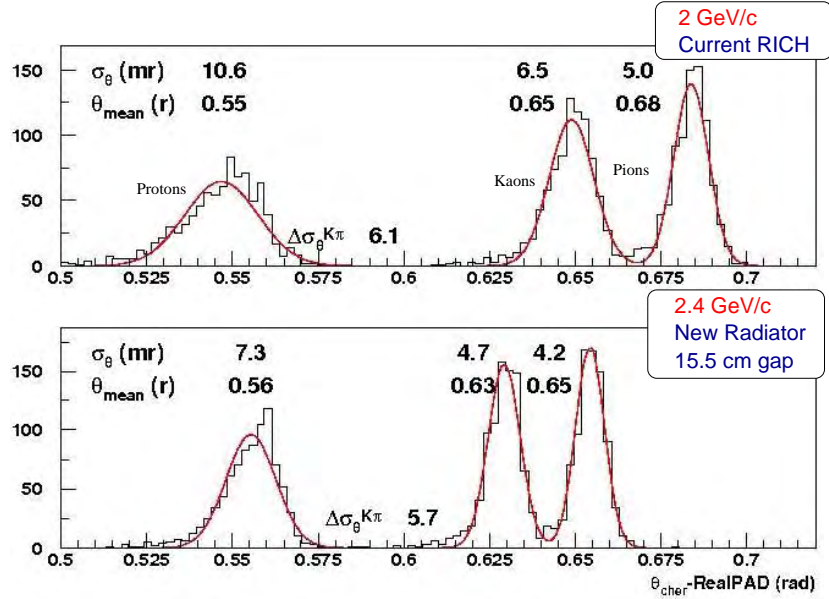


Figure 15: Monte Carlo simulation of the RICH performance: reconstructed Čerenkov angle for equally populated p, K and π samples. Top: the existing RICH at 2 GeV/c (normalized to the measured values); bottom: the projected performance at 2.4 GeV/c after the radiator and proximity gap upgrade.

with aerogel A1 and A2 will provide a π^+/K^+ separation with proper redundancy for this experiment. Although the design details are not finalized yet, the estimated cost is at \$50k.

Since the RICH detector has demonstrated good performances during E94-107 experiment and its upgrade is reasonably simple and inexpensive, we prefer the RICH detector as our first option. Target single-spin asymmetries from positively identified charge kaons in SIDIS or exclusive kaon production provide valuable by-products of this experiment.

3.7 Trigger and offline event selection

A coincidence time window of 50 ns will be enough to form the coincidence trigger. Trajectory corrected time-of-flight resolution is expected to be better than 2 ns. The raw accidental coincidence rate will be at 20-30 Hz. After the BigBite calorimeter ADC cut and the HRS_L PID cut, accidental coincidence events are not expected to survive at any significant level. Two-arm vertex consistency cut is expected to further eliminate the accidental events by an extra factor of 10, if there are any left. The true $(e, e'\pi^+)$ coincidence rate is expected to be at 1.0-1.5 Hz level. The above values are summarized in Table 5

Table 5: Expected accidental rates

Selection	Rate [Hz]	Mode
Coincidence Window (50 ns)	20-30	Online
AND PreShower + Shower (BB and HRS)	2-3	Online
AND PreShower + Shower (BB and HRS)	0.2	Offline
AND Under the coincidence TOF peak	2.0×10^{-2}	Offline
AND Vertex Consistency	2.0×10^{-3}	Offline

3.8 Luminosity monitors

The HAPPEX experiments E99-115 and E00-114 have recently completed an extended run. These experiments built 8 luminosity monitors called the Lumis. Each detector is made of Quartz with an air light guide. The monitors are placed downstream of the target within the beam pipe at a scattering angle of $7mrad$, see Fig. 16. The Lumis have performed very well during HAPPEX, monitoring the Luminosity to a very high precision of the 30 Hz beam helicity flips.

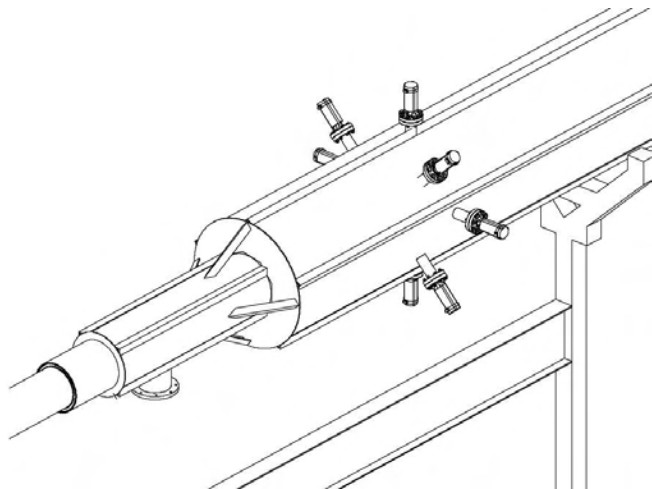


Figure 16: The Hall A Lumis in the beam pipe downstream of the target.

For this experiment, the target spin will be flipped in a time period of fifteen to thirty minutes. To study the systematic effects of the Lumis in this time window, the data HAPPEX slug 30 was examined. This slug consisted of fourteen runs, each of 56 minutes in length. The data for each run was divided into four equal length time periods. The results from all eight Lumis were summed to remove Physics effects. Each sum was divided by the value from the Hall A beam charge monitor (BCM) to cancel beam jitter. The average result was determined for each 14 minute sequence. The only cut used required a non-zero beam current. The basic asymmetry assuming an ABAB sequence for all is 5×10^{-6} . To get a better handle on the systematic error a random number generator was used to randomly determine either an ABBA or BAAB pattern for each run. The 14 sequences were randomly determined 1000 times giving a root mean square of 5×10^{-5} as

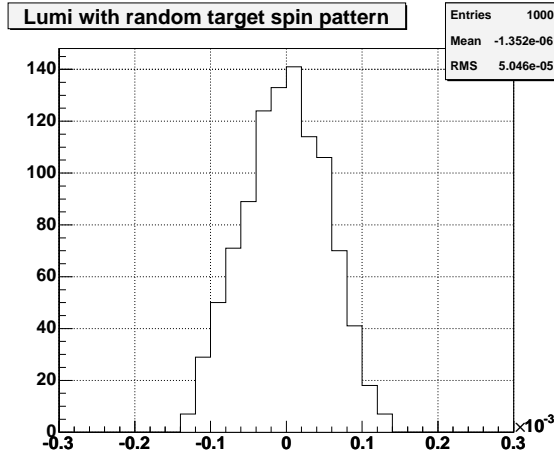


Figure 17: The Asymmetries of the Hall A Lumi sum divided by the BCM with 14 minute time windows for HAPPEX slug 30, using 1000 different random combinations of ABBA or BAAB. The very high rate of HAPPEX experiments means that the RMS is related only to the Lumi systematic error for 14 minute time windows.

shown in Fig. 17.. The HAPPEX data has a very large data rate so all errors should be systematic. This test has shown that the Lumis should be able to monitor the luminosity differences between target spin up and target spin down for the vertically polarized single spin ^3He experiments to the 5×10^{-5} level.

3.9 The polarized ^3He target

The Hall A polarized ^3He target [41] was successfully used in it's standard configuration for the experiments E94-010 [42] and E95-001 [43] in 1998-1999, E99-117 [44], E97-103 [45] in 2001, E01-012 [46] and E97-110 [47] in 2003.

The standard polarized ^3He target used optically pumped Rubidium vapor to polarize ^3He nuclei via spin-exchange. Two sets of Helmholtz coils provided a 25 Gauss holding field for any direction in the scattering (horizontal) plane. Target cells were up to 40 cm long with density of about 10 amg (10 atm at 0°). Beam currents on target ranged from 10 to 15 μA to keep the beam depolarization effect small and the cell survival time reasonably long (> 3 weeks). The luminosity was about 10^{36} nuclei/s/cm 2 . The in-beam average target polarization achieved was typically over 40%. Two kinds of polarimetry, NMR and EPR (Electron-Paramagnetic-Resonance), were used to measure the polarization of the target. The uncertainty achieved for each method was less than 4% relative and the methods agreed well within errors.

Recent development effort for the approved polarized ^3He experiments, (E02-013, G_E^p [37] and E03-004 transversity) has achieved a number improvements. Most significant is the success of the K-Rb hybrid spin-exchange technique [48]. Due to the much higher K- ^3He spin exchange efficiency, the new hybrid cells have significantly shorter spin-up times and improved performance. There are about 10 usable hybrid cells manufactured by the UVa (Gordon Cate's) group and the William and Mary (Todd Averett's) group. Most of the

cells have spin-up times of 6-8 hours (to be compared with 20 hours for a typical Rb cell) and polarizations without beam of 45 – 50% (to be compared with 40 – 45% for a typical Rb cell). Also due to the improved spin exchange efficiency, the recent testing results indicate that only about 2/3 of the laser power is needed to achieve the maximum polarization. The success rate of cell manufacturing is also greatly improved since with the much short spin-up time, the requirements on the cell life-time become significantly relaxed.

A new laser building next to the counting house was constructed earlier this year to replace the laser hut in the hall. A new target lab with its infrastructure and safety interlock system has been setup in the new laser building. A new target system (for the G_E^n experiment) has been setup and is being tested in the new target lab. With the laser building moved outside the hall, an optical fiber system is needed to transport the laser light into the hall. Eight 75m-long optical fibers and two 5-to-1 combiners were acquired and tested. The typical light intensity drop through the optical fiber system is about 15%. Air cooling and a temperature interlock system are used to protect the fibers from over-heating. Eight Coherent 30 watts diode laser FAP-system were used for previous experiments (three for longitudinal polarization, three for transverse polarization and two spares). Four of the used Coherent lasers have recently replaced the diodes. Two additional Coherent 60 watts diode laser DUO-FAP were purchased recently. There should be enough lasers and optical components for the next a few planned polarized ^3He experiments. including this proposed measurement.

This experiment requires frequent polarization direction reversal to minimize target-spin-correlated systematic uncertainties. Studies have been performed on this issue. The target spin will be flipped using RF AFP technique and the laser polarization flip will be accomplished with rotating quarter-wave plates. Using AFP RF spin-flip technique, polarization direction reversal was achieved in a time scale of a few seconds. A rotation stage was acquired and was tested to be able to rotate the quarter-wave plate also in a time scale of a few seconds. Due to AFP polarization loss, the maximum polarization will be reduced for frequent spin-flip. The equilibrium polarization P_{eq} is related to the maximum polarization P_{max}

$$P_{eq} = \frac{T_{flip}}{T_{flip} + \delta T_{spin-up}} P_{max}, \quad (18)$$

where T_{flip} and $T_{spin-up}$ are the spin-flip time and the spin-up time correspondingly. δ is the AFP polarization loss for each spin-flip. The frequency of the polarization reversal will be kept to be around 15-30 minutes. It is optimized to keep the maximum polarization while still have target-spin-correlated systematic uncertainties under control. With a spin-flip frequency of 15-30 minutes, a spin-up time of 6 hours, and an AFP loss of 0.3%, the maximum equilibrium polarization will be reduced by 5 – 10% relative (i.e. instead of 45 – 50%, it will be 42 – 47% for a 15 minutes flip or 43 – 48% for a 30 minutes flip).

For this measurement, a third set of Helmholtz coils is needed to provide a holding and polarization field in the vertical direction. It will be added without taking apart the existing sets of coils. Fig. 18 shows the conceptual design.

To accommodate optical pumping in the vertical direction, the oven will be tilted to be offset from the center so that the laser light will not overlap with the vertical motion

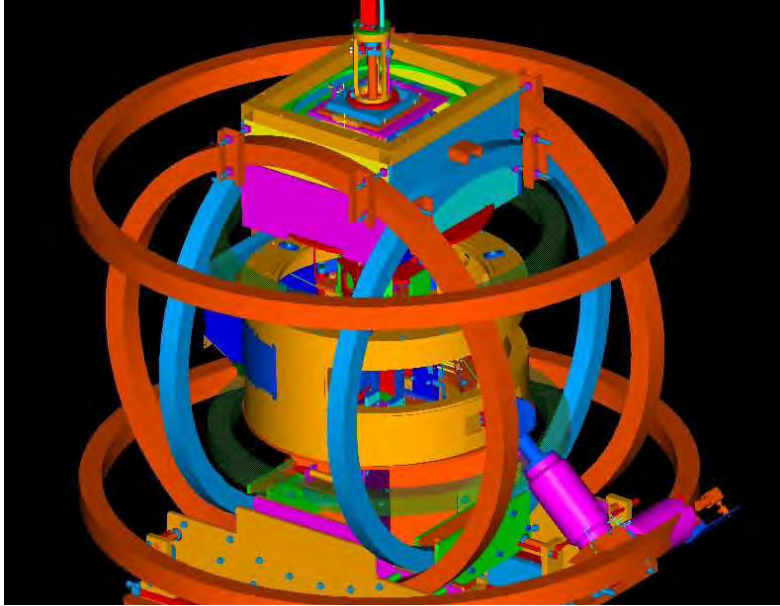


Figure 18: The design of the vertical coils for the polarized ^3He target.

and support mechanism. A mirror will be mounted on top of the pumping chamber to allow the laser light to be reflected into the pumping chamber from the top.

3.9.1 Effects of BigBite magnetic field

The BigBite magnet will be 1.5 meters away from the target center. Its fringe field can cause a field gradient in the target region. A field clamp will be used to reduce the field gradient. A set of correction coils will be used to further minimize the field gradient. From the experience of running an earlier polarized ^3He experiment E97-110 (Small Angle GDH), which had a significant fringe field from a Septum magnet, using of a field clamp and correction coils reduced the field gradient by an order of magnitude to eliminate possible complications. The BigBite fringe field at the target region is significantly less than that of the Septum in the first run-period of E97-110. The field gradient after the correction is expected to be less than 10 mG/cm, which has a negligible effect on the polarization and a reasonably small effect on the AFP loss.

4 Event Rate Estimate and Statistical Uncertainties

4.1 Cross section and rate estimate

The estimation of the coincidence cross sections has the following inputs:

- The inclusive $p(e, e')$ and $n(e, e')$ cross sections. Deep-inelastic cross sections for ^3He are assumed to be the sum of the two protons plus one neutron, neglecting the nuclear effects in the intermediate x -region.

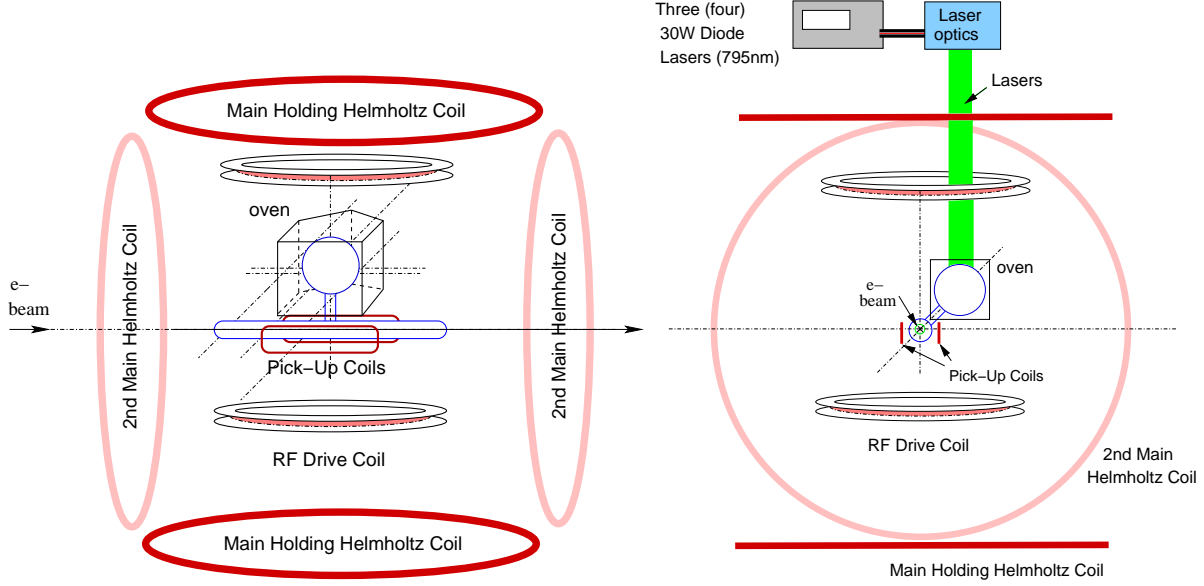


Figure 19: The schematic of the polarized ^3He target, side view (left) and beam view (right).

- A parameterization of $R = \sigma_L/\sigma_T$ to account for the longitudinal photon polarization.
- Parameterizations of the fragmentation functions D_π^+ and D_π^- for quark to pion fragmentation, D_K^+ , D_K^- and D_d^K for quark to kaon fragmentation.
- A model of the transverse momentum distributions of pion and kaon as fragmentation products.

The inclusive deep inelastic (e, e') cross section can be expressed in the quark parton model as:

$$\frac{d^2\sigma}{d\Omega dE'} = \frac{\alpha^2(1 + (1 - y)^2)}{sxy^2} \frac{E'}{M_N \nu} \sum_{q, \bar{q}} e_q^2 f_1^q(x), \quad (19)$$

where $s = 2EM_N + M_N^2$. The unpolarized quark distribution functions $f_1^q(x)$ and $f_1^{\bar{q}}(x)$ are taken from the CTEQ5M global fits [49]. The semi-inclusive ($e, e'h$) cross section relates to the quark fragmentation function $D_q^h(z)$ and the total inclusive cross section σ_{tot} through:

$$\frac{1}{\sigma_{tot}} \frac{d\sigma(e, e'h)}{dz} = \frac{\sum_{q, \bar{q}} e_q^2 f_1^q(x) D_q^h(z)}{\sum_{q, \bar{q}} e_q^2 f_1^q(x)}. \quad (20)$$

For the quark to pion fragmentation functions $D_\pi^+(z)$ and $D_\pi^-(z)$, we follow the parameterization [50] of KKP to obtain the sum of $D_\pi^+(z) + D_\pi^-(z)$. For the ratio $D_\pi^-(z)/D_\pi^+(z)$, we use a fit to the HERMES data [51]: $D_\pi^-/D_\pi^+ = (1 - z)^{0.084}/(1 + z)^{1.984}$. Fragmentation functions D_K^+ , D_K^- and D_d^K in the KKP parameterization are used.

Existing data indicate that the fragmented products follow a Gaussian-like distribution in transverse momentum. For the $N(e, e'\pi)X$ reaction, recent HERMES preliminary data showed that the transverse momentum (P_\perp) distribution for both π^+ and π^- follow the form of $e^{(-aP_\perp^2)}$ with $a = 3.76 \text{ (GeV/c)}^{-2}$, corresponding to an average quark transverse momentum of $\langle P_\perp^2 \rangle = 0.26 \text{ (GeV/c)}^2$. Charged kaon transverse momentum distributions are also found to be similar. We used this distribution and realistic spectrometer acceptances in a Monte Carlo simulation to estimate the count rates. The issue of hadron decay is also considered in the rate estimation. The typical survival factors for π^\pm and K^\pm of 2.40 GeV/c momentum are 0.83 and 0.25, respectively, after a flight-path of 25.0 meters through HRS.

4.2 Cross sections, rates and total number of $(e, e'\pi^+)$ events

The cross sections, event rates and total number of events for each bin are listed in Table-6 for the $(e, e'\pi^+)$ reaction. We have assumed a beam current of 15 μA , a target length of 40 cm with 10 amgs of ^3He gas and a target polarization of 42%.

E' GeV	$\Delta E'$ GeV	θ_e deg.	$\langle x \rangle$	$d\sigma_{(e,e')}$ nb/GeV/sr	$d\sigma_{(e,e'\pi^+)}$ nb/GeV ² /sr ²	Rate _{π^+} Hz	N_{π^+} k
					$\theta_\pi = 16.0^\circ, p_\pi = 2.4 \text{ GeV/c}$		
0.815	0.431	30.0	0.135	29.64	8.17	0.24	461.0
1.246	0.398	30.0	0.225	19.37	7.19	0.20	374.5
1.612	0.340	30.0	0.315	12.95	5.53	0.13	246.1
1.925	0.381	30.0	0.405	8.37	3.63	0.10	181.0

Table 6: Cross sections, event rates and the total number of events (N_{π^+} in thousands). Data of all x -bins will be collected simultaneously.

Physics asymmetries from ^3He are translated into neutron asymmetries $A_{UT}^{\pi^+}(n)$ and are listed in Table 7 together with the corresponding dilution factors. An effective neutron polarization of 86.5% in ^3He ground state has been taken into account.

E' GeV	$\langle x \rangle$	R	$B(x)/A(x, y)$	D_{nn}	z_π	f_{π^+}	$1/f_{\pi^+} P_T P_n \sqrt{N_{\pi^+}}$ %
0.815	0.135	0.32	0.249	0.267	0.46	0.27	1.50
1.246	0.225	0.26	0.375	0.398	0.51	0.23	1.93
1.612	0.315	0.21	0.485	0.501	0.55	0.20	2.77
1.925	0.405	0.18	0.584	0.582	0.59	0.18	3.69

Table 7: The expected statistical uncertainties of the single spin asymmetry $A_{UT}^{\pi^+}(n)$ are listed with the corresponding dilution factors f_{π^+} , $R = \sigma_L/\sigma_T$, and the Collins kinematic factor $B(x)/A(x, y)$. The ideal Collins kinematic factor D_{nn} are also listed for comparison.

4.3 Statistical uncertainties of Collins and Sivers moments

With a full 2π coverage of the Collins angles and almost 2π coverage of Sivers angle, this experiment can make clear separation of Collins asymmetries from Sivers asymmetries. For each kinematic bin, we need to find the best fit of parameters a and b for an event-probability distribution:

$$y_i(\phi_h^i, \phi_S^i) = \frac{1}{NV(\phi_h^i, \phi_S^i)} \left[1 + a \sin(\phi_h^i + \phi_S^i) + b \cdot \sin(\phi_h^i - \phi_S^i) \right] \quad (21)$$

in which N is the number of event. The relative phase space volume $V(\phi_h^i, \phi_S^i)$ can be obtained from target-spin-averaged counts. The details of asymmetry separations and statistical uncertainties are provided in Appendix-II.

The expected statistical uncertainties on the overall target SSA $A_{UT}^{n\pi^+}$, and separated into the Collins asymmetry $A_{UT}^{n\pi^+Collins}$ and the Sivers asymmetry $A_{UT}^{n\pi^+Sivers}$ are listed in Table 4.3 for the $n^\uparrow(e, e'\pi^+)$ measurements.

$\langle x \rangle$	$\delta A_{UT}^{n\pi^+}$ %	$\delta A_{UT}^{n\pi^+Collins}$ %	$\delta A_{UT}^{n\pi^+Sivers}$ %
0.135	1.50	2.61	2.61
0.225	1.93	2.95	2.95
0.315	2.77	3.96	3.96
0.405	3.69	5.20	5.20

As by-products, target SSA in $n^\uparrow(e, e'K^+)$ reaction will also be measured. The corresponding total number of events, dilution factors and statistical uncertainties on $A_{UT}^{nK^+}$, and uncertainties of its Collins and Sivers moments are listed in Table. 8.

$\langle x \rangle$	f_{K^+}	N_{K^+} k	$\delta A_{UT}^{nK^+}$ %	$\delta A_{UT}^{nK^+Collins}$ %	$\delta A_{UT}^{nK^+Sivers}$ %
0.135	0.28	67.7	3.77	6.56	6.56
0.225	0.24	53.8	4.86	7.44	7.44
0.315	0.21	36.3	6.87	9.83	9.83
0.405	0.18	27.7	9.08	12.80	12.80

Table 8: The expected number of events (N_{K^+}) in $(e, e'K^+)$ channel, the corresponding dilution factor f_{K^+} , statistical uncertainties of $A_{UT}^{nK^+}$, and statistical uncertainties of Collins and Sivers moments of K^+ production on a neutron.

4.4 Systematic uncertainties

The experimental uncertainties on SSA will be dominated by statistical uncertainties. We discuss several possible sources of systematic uncertainties in this section.

4.4.1 Effective nucleon polarization in ${}^3\text{He}$

Effective nucleon polarization in ${}^3\text{He}$ for deep-inelastic scattering gives:

$$g_1^{3He} = P_n g_1^n + 2P_p g_1^p \quad (22)$$

where $P_n(P_p)$ is the effective polarization of the neutron (proton) inside ${}^3\text{He}$ [52]. These effective nucleon polarizations $P_{n,p}$ can be calculated using ${}^3\text{He}$ wave functions constructed from N-N interactions, and their uncertainties were estimated using various nuclear models [53, 52, 54, 55], giving

$$P_n = 0.86_{-0.02}^{+0.036} \quad \text{and} \quad P_p = -0.028_{-0.004}^{+0.009}. \quad (23)$$

The small proton effective polarization (2.8%) causes small offsets in the ${}^3\text{He}$ asymmetries, compared to that from a free neutron. The uncertainties associated with this small offset are even smaller when considering that the corresponding proton asymmetries are relatively well known from the HERMES data.

4.4.2 Corrections to A_{UT} due to target polarization drifts

The systematic uncertainties due to the target polarization measurements contribute to $\pm 4\%$ relative uncertainties to the systematics of A_{UT} .

The target polarization between spin up and spin down runs may not be exactly the same. A drift in the target polarization does not cause any single-spin asymmetry itself, but results in a small change which is easy to correct. Assuming the yield is: $\sigma = \sigma_0 + P_T \sigma_1$ for target spin up and spin down, we have: $\sigma_+ = \sigma_0 + P_T \sigma_1$ and $\sigma_- = \sigma_0 - P_T \sigma_1$. The measured asymmetry is:

$$A_0 = \frac{\sigma_+ - \sigma_-}{\sigma_+ + \sigma_-} = P_T \frac{\sigma_1}{\sigma_0}. \quad (24)$$

If during spin down runs the average target polarization changes to $P_T + \delta P_T$, such that $\sigma'_+ = \sigma_0 + P_T \sigma_1$ and $\sigma'_- = \sigma_0 - (P_T + \delta P_T) \sigma_1$, the measured asymmetry changes to:

$$A' = \frac{\sigma'_+ - \sigma'_-}{\sigma'_+ + \sigma'_-} = A_0 \frac{1 + \frac{\delta P_T}{2P_T}}{1 - \frac{\delta P_T}{2P_T} \cdot A_0}. \quad (25)$$

Since $A_0 \delta P_T / 2P_T \ll 1$, we have:

$$A' \approx A_0 \left(1 + \frac{\delta P_T}{2P_T}\right) \left(1 + \frac{\delta P_T}{2P_T} \cdot A_0\right) \approx A_0 \left(1 + \frac{\delta P_T}{2P_T}\right). \quad (26)$$

As long as the target polarization is measured, the drifts in average polarization between spin up and spin down runs will not cause any significant uncertainty in A_{UT} .

4.4.3 Pions from exclusive ρ production

Pions from exclusive ρ production can be a possible source of contamination. However, at the kinematics of this experiment such contaminations are negligible. Recent Hall C E00-108 experiment [56], which run at a similar kinematics as this experiment, has estimated the exclusive ρ contributions to the SIDIS cross section, the results are shown in Fig. 20, the difference between open symbols and filled symbols (ρ contribution subtracted) are very small at $z \approx 0.5$.

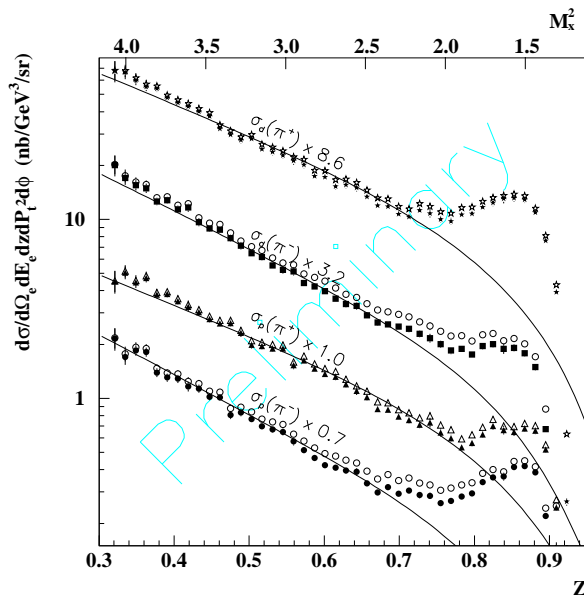


Figure 20: Hall C E00-108 experiment [56], the difference between open symbols and filled symbols corresponds to exclusive ρ contribution.

4.4.4 Other terms in SSA and cross sections

The $\sin(3\phi_h - \phi_S)$ term in Eq. 5 is expected to be rather small since it involves not only transverse-momentum-dependent distribution functions ($h_{1T}^{\perp q}$) but also the Collins fragmentation functions (H_1^\perp). The coverage of ϕ_h in this experiment is close to 180° for most x -bins, therefore, we expect all $2\phi_h$ and $3\phi_h$ terms to be averaged out nicely. Any significant angular dependence (such as $\cos(2\phi)$ terms) of spin independent cross sections can be easily identified and corrected for within the experimental acceptance. The experimental phase space in ϕ_h can be determined from a Monte Carlo simulation cross checked with uncorrelated single-arm events.

5 Beam time request, hardware costs and installation time needed

5.1 Beam time request

The beam time request are listed in Table 9. We request 576 hours (24 days) of total beam time, of which 528 hours is for beam on the polarized ^3He target. A total overhead time of 48 hours is requested. This overhead time can be shared between activities such as unpolarized target runs, target spin flip and target polarization measurements, as has been done in the past during other Hall A polarized ^3He target experiments. Major target related down times can also be arranged to coincide with the scheduled accelerator maintenance activities in order to save overhead time.

Table 9: Beam time request.

	Time (Hour)
Production on Pol. ^3He	528
Reference cell runs, optics and detector check	16
Target Overhead: spin rotation, polarization measurement	32
Total Time Request	576 (24 days)

Table 10: Details of the beam time request.

5.2 Hardware costs and installation time needed

All major hardware components required in this experiment, including the target, spectrometers and detectors are either already standard Hall A equipments or about to become the standard Hall A equipments. The BigBite spectrometer together with its electron detection package is scheduled to be commissioned in February 2006 for the G_{En} experiment. This proposal has no additional requirement on the BigBite detectors beyond its expectation for the G_{En} experiment.

The vertical target magnet coils, together with a new oven for pumping cell, mechanical support, laser optics and new target cells add up the cost to be about \$100 k.

The overall installation time needed for this experiment is estimated to be between four to six weeks. Installation of the Hall A polarized ^3He target can be accomplished within two to three weeks. The installation time needed for the BigBite spectrometer, depends on the sequence of experiments, can be two to three weeks.

Since this proposed ($e, e'\pi^+$) measurement will use exactly the same setup and instrumentation as in the approved E03-004 ($e, e'\pi^-$) measurements, the change-over time is less than 2 hours if scheduled to run in sequence.

6 Expected Results

6.1 Neutron asymmetry $A_{UT}^{n\pi^+}$, Collins and Sivers moments

The expected statistical accuracies of Collins and Sivers moments (as defined in Eq. 10-11) of neutron are plotted in Fig. 21. HERMES [12] and COMPASS [13] A_{UT} data are also shown as a comparison.

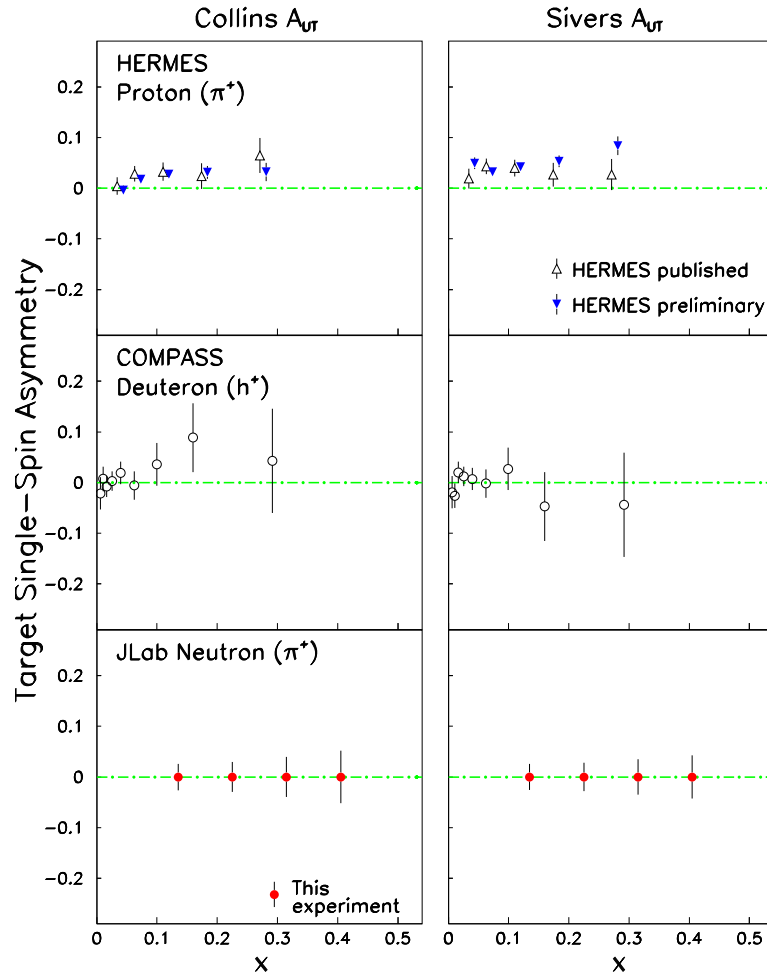


Figure 21: The projected JLab data of target single spin asymmetry A_{UT} for both Collins and Sivers asymmetries in $n^\uparrow(e, e'\pi^+)$ reaction are compare with HERMES [12] and COMPASS [13] A_{UT} data.

Collins moments of neutron in $n^\uparrow(e, e'\pi^+)$ reaction are compared with the parameterization of Vogelsang and Yuan [34, 35] in Fig. 22. Since Vogelsang and Yuan [34] concluded that $H_1^{\perp fav} \approx -H_1^{\perp unfav}$, they predicted a rather small asymmetries due to the cancellations between u and d -quarks. A PQCD model calculation [18] of Ma Schmidt and Yang are plotted in Fig. 22 in which it was assumed that the unfavored and the favored Collins functions follow $H_1^{\perp unfav} / H_1^{\perp fav} \approx D_1^{unfav} / D_1^{fav}$. With this experiment providing one of

the the first direct neutron data together with E03-004 of $n^\uparrow(e, e'\pi^-)$ reaction, a combined analysis with the HERMES proton data using all four types of the Collins asymmetries will be able to completely constrain four unknowns: quark transversity δu and δd and Collins fragmentation functions $H_1^{\perp fav}$ and $H_1^{\perp unfav}$.

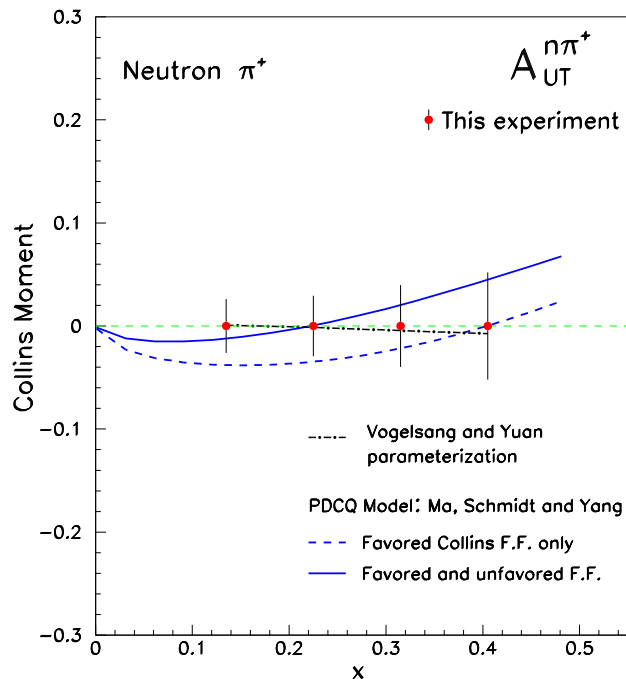


Figure 22: The projected JLab data of neutron Collins moments are compared with the parameterization of Vogelsang and Yuan [34, 35] and model predictions of Ma, Schmidt and Yang [18].

Sivers moments of neutron in $n^\uparrow(e, e'\pi^+)$ reaction are compared with the parameterization of Anselmino *et al.* [32] and Vogelsang and Yuan [34, 35] in Fig. 23. Both parameterization predict rather large Sivers moments of $A_{UT}^{n\pi^+}$ with large uncertainties, reflecting the fact that the existing HERMES and COMPASS data do not constrain d -quark Sivers function well enough. A measurement of neutron Sivers asymmetry can certainly fill in our knowledge gap. In a simplified manner, we have the Sivers $A_{UT}^{n\pi^+} \propto 4f_{1T}^{\perp(1)d} \cdot D_1^{fav} + f_{1T}^{\perp(1)u} \cdot D_1^{unfav}$. At the kinematics of this experiment, the regular fragmentation functions are well-known and the ratio is $D_1^{unfav}/D_1^{fav} \approx 1/3$. Therefore, for this experiment we have Sivers $A_{UT}^{n\pi^+} \propto 4f_{1T}^{\perp(1)d} + \frac{1}{3}f_{1T}^{\perp(1)u}$. If the Sivers $A_{UT}^{n\pi^+}$ turns out to be negative, opposite to the sign of the proton Sivers $A_{UT}^{p\pi^+}$ following our expectation based on the HERMES data, a large d -quark Sivers function opposite to that of u -quark is needed. This will indicate that the d -quark carries a rather large angular momentum opposite to the nucleon spin. If on the other hand the Sivers moment $A_{UT}^{n\pi^+}$ turn out to be positive, a significant inconsistency will pose a strong challenge to the existing theoretical framework for the Sivers effect. Clearly, neutron measurements in $n^\uparrow(e, e'\pi^+)$ reaction are urgently needed. A combined analysis of E03-004 and this experiment will provide the

flavor decomposition of Sivers functions.

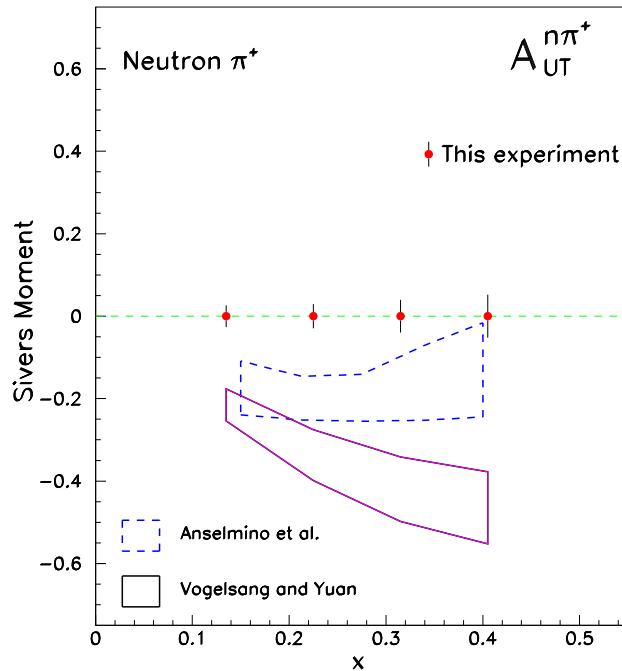


Figure 23: The projected JLab data of neutron Sivers moments are compared with the parameterization of Anselmino *et al.* [32] and Vogelsang and Yuan [34, 35]. The asymmetries are expected to be large and negative.

6.2 SSA in SIDIS electroproduction of Kaons

The study of kaon production gives direct sensitivity to s -quark and \bar{s} -antiquark distributions. Inclusive and semi-inclusive asymmetries for the production of positive and negative charged pions and kaons from a longitudinally polarized deuteron target were measured by the HERMES collaboration recently. A “leading-order” QCD analysis was carried out [57] for these data together with the reanalysis of the previous HERMES asymmetry data on inclusive and semi-inclusive production of charged pions from a longitudinally polarized hydrogen target. The HERMES collaboration extracted the flavor-separated quark helicity distributions and all extracted sea quark polarizations are consistent with zero.

Single spin asymmetry from semi-inclusive production of positively charged kaons at the proposed DIS kinematics from a transversely polarized ^3He target will be obtained simultaneously with π^+ . Fig. 24 shows the projected statistical errors on $A_{UT}^{K^+}$ as a function of x from the transversely polarized “neutron”. For comparison, the projection on $A_{UT}^{K^-}$ which will be obtained from the approved π^- experiment (E03-004) is also shown. While currently there is no theoretical prediction for the kaon SSA, this set of data will be obtained for “free” and will motivate future work in flavor, valence/sea quark separation of the quark transversity distributions.

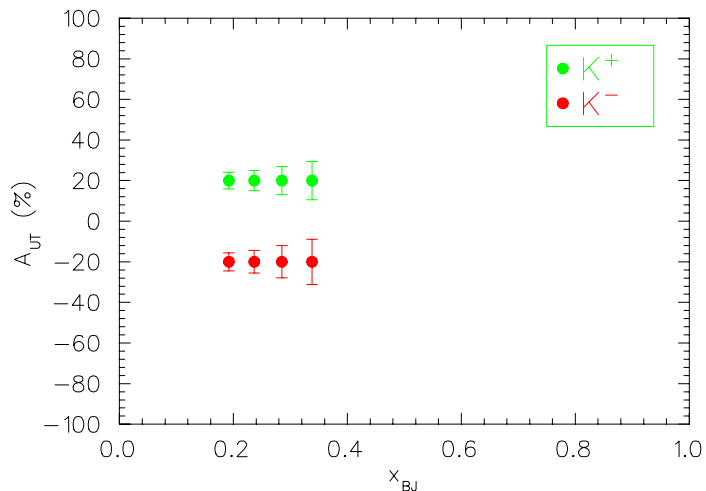


Figure 24: Projected statistical errors of A_{UT}^n for SIDIS production of kaons from the “neutron” using a polarized ^3He target, K^+ from this experiment and K^- from experiment E03-004.

7 Relation with other experiments

- Hall A E03-004 $n^\uparrow(e, e'\pi^-)$.

The proposed experiment is a twin experiment of the Hall A E03-004 $n^\uparrow(e, e'\pi^-)$ experiment. The combined measurements of π^+ and π^- at the same DIS kinematics will allow the study of the surprising feature suggested by the comparison between the HERMES π^+ and π^- results obtained from a transversely polarized proton target.

- The HERMES experiment.

The HERMES results on SSA from DIS electroproduction of charged pions were obtained from a transversely polarized proton target. Interesting features have been observed by comparing results between the negatively and positively charged pions, particularly in the case of the extracted Sivers moment. It is essential to carry out charged pion measurements from a transversely polarized neutron target (^3He target) as proposed by this experiment and the twin experiment on π^- , in the similar x range as that of the HERMES.

- The COMPASS experiment

The reported results on both the Collins and Sivers asymmetry from COMPASS were obtained from a transversely polarized deuteron target. The COMPASS collaboration plans to carry out similar measurements from a transversely polarized proton target in the future. By combining the COMPASS deuteron results and future proton results, one can extract Sivers and Collins asymmetries from the neutron. However, the COMPASS x range is rather low with the highest x value

being around 0.1, therefore the COMPASS experiment is complementary to the proposed experiment.

- Belle on Collins fragmentation function

The Collins asymmetry determined from the SSA of SIDIS electroproduction of pions contains information on both the unknown quark transversity distribution and the unknown Collins fragmentation function. The chiral-odd Collins fragmentation function can be determined from the $e^+e^- \rightarrow \pi^+\pi^-X$ process and the Belle data are currently being analyzed in order to extract the Collins fragmentation function. The extracted Collins fragmentation function will be important to the determination of the quark transversity from the Collins asymmetry measured from the SIDIS electroproduction of pions as proposed in this experiment. Therefore the Belle measurement of the Collins function is important and complementary to this experiment.

- Transversity at RHIC

The transversity distribution for the valence quark in the proton can be studied at RHIC at the center of mass energy of 200 GeV through the Drell-Yan process: $\vec{p} + \vec{p} \rightarrow l^+l^-X$. The RHIC Drell-Yan measurements allow relatively clean determination of the valence quark transversity though the corresponding x range is lower than that of the proposed experiment.

- The PAX experiment

The PAX collaboration [58] proposed to carry out a first measurement of the transversity distribution of the valence quarks in the proton by the Drell-Yan process with transversely polarized anti-proton beam and a transversely polarized proton internal gas target. The proposed experiment will take place at the FAIR facility at GSI. The design of the PAX detector is optimized for the detection of the Drell-Yan lepton (electron-positron) pairs for the transversity measurements. The Phase-I physics program at FAIR GSI could start in 2014 and the transversity program is planned for Phase-II. The polarized \vec{p} - \vec{p} Drell-Yan measurements are complementary to SIDIS measurements as proposed. Results from the PAX experiment will not become available in quite some time.

- CLAS longitudinal SSA

The CLAS collaboration determined SSA from SIDIS electroproduction of charged pions from a longitudinally polarized proton target, which is not directly related to the proposed measurements from a transversely polarized ^3He target.

- JLab at 12 GeV

The proposed experiment together with its twin experiment will open a new window at JLab in the study of the quark transversity. The success of the 6 GeV experiments will be essential for the success of the future JLab 12 GeV program on transversity.

Probing quark transverse polarization is among the goals of several ongoing and future experiments because it is the least known leading-twist quark distributions. The experimental study of transverse polarization distributions, which is now only at its inception, promises to have a very exciting future. Understanding the transversity distributions for different quark flavors is certainly a complex task which demands major efforts in different laboratories in studying many different processes ranging over a wide kinematic region.

This is a fast evolving field with growing interest worldwide. It is important for JLab to be a major player in this important frontier. Running the proposed experiment at the current maximum machine energy of CEBAF is crucial because it will impact the success of the future 12 GeV JLab program on transversity. It will also have impact on other related programs and particularly on the design of future facilities with transversity study as one of their important physics goals, for example the e-RHIC and the J-PARC. The proposed 6 GeV experiment will also help to move theory forward in understanding and in modeling the quark transversity distributions. Therefore, it is essential to run the proposed experiment NOW.

8 Summary

We are proposing a first measurement of SSA from semi-inclusive electroproduction of positive pions from a transversely polarized ^3He target in DIS region. The proposed experiment together with the approved Hall A experiment on negative pions will provide data for the first time on the Collins and Sivers asymmetry from the neutron. These data together with the HERMES results from a transversely polarized proton target in the similar x region and the COMPASS results from a transversely polarized deuteron target will provide powerful constraints on the transversity distributions on both u -quark and d -quark in the valence region. The proposed experiment will open up a new window at JLab for the study of the quark transversity distribution and will be important for the future experimental program on transversity study with a 12 GeV CEBAF at Jefferson Lab.

To carry out the experiment, we will use the left-arm HRS spectrometer, and the BigBite Spectrometer configured in the same way as that for the G_E^n experiment, which will run in early 2006. We will use the Hall A polarized ^3He target by adding a new pair of Helmholtz coils for this experiment.

We request a total number of 24 days of beam time at an incident electron beam energy of 6 GeV.

9 Acknowledgments

We thank W. Vogelsang and F. Yuan, M. Anselmino and A. Prokudin for providing calculations of their parameterizations for the kinematics of the proposed measurements.

A Appendix-I. Simulation of BigBite background rates and comparisons with test runs

We used a GEANT3 based simulation code [38] to study the background rates on BigBite detectors. The event generator uses photon-nuclear fragmentation package DINREG to substitute the original code PFIS. The electron-nuclear interactions are modeled using equivalent photon representation of an electron [38]. The same simulation code was used earlier for many JLab experiments to address issues related to background rates. The simulation code usually tends to over-estimate background rates by a factor of 2-3.

We compared background rate data in three experimental situations with the simulation. After confirming the reliability of the simulation, we extended our background simulation to the situation of BigBite detectors in the G_E^n experiment and in the “neutron transversity” experiment.

The first comparison with data is for a BigBite test run taken in April, 2005, during the Short Range Correlation (SRC) experiment. The beam was 4.63 GeV at a current of $2 \mu\text{A}$. The target was a 4 cm LD_2 cell. The BigBite is located at 99° , 1.0 meter away from the target. The BigBite magnetic field was 0.986 T in negative mode. The simulation reproduce rates on three different scintillator planes to within 50%, for both cases of magnet on (Fig. 25) and magnet off (Fig. 26).

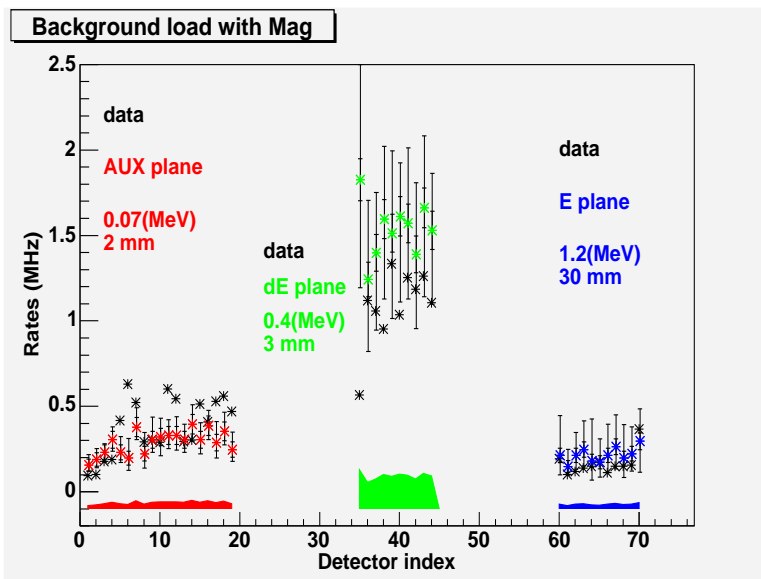


Figure 25: Rates comparison between test data and simulation with BigBite magnet turned on during the SRC experiment. Scintillator thickness and cut offs in simulated energy deposit are indicated for each plane. The points with error bars are from the simulator. The inner error bars show the statistical uncertainty of the simulation. The outer error bars correspond to the systematics uncertainty due to the threshold cuts in the test data analysis. The color bands show the systematics due to the uncertainties of the geometry.

The second comparison is between the SRC production data and the simulation. The

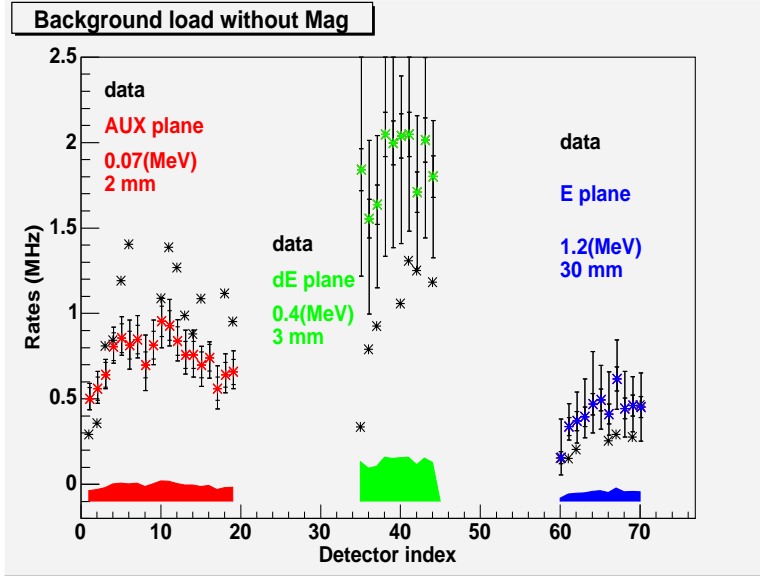


Figure 26: Simulation compare with test run rates. Same as in Fig. 25, but with the BigBite dipole magnet turned off.

beam energy was 4.6 GeV and the current was $8.2 \mu\text{A}$. The target was a tilted Carbon foil with a thickness of 42.3 mg/cm^2 . BigBite is at 99 degrees with 1.0 meter drift distance. The background rates from data is 70 kHz. The simulation result is $181.6 \pm 7.6(\text{stat}) \pm 30.5(\text{sys}) \text{ kHz}$. The systematic error include uncertainties in geometry, threshold cuts, etc. The simulation overestimate the rates by a factor of two.

The third comparison is between a BigBite wire chamber test run and the simulation. The beam energy was 2.75 GeV and the current was $8 \mu\text{A}$. Only the first wire chamber was used in the test run without any magnet. The chamber was located at 70 degree at a distance of 10 meter. The data showed a background rates of 1.8 kHz/wire. At a cut of 1 keV for energy deposit on the wire chamber, the simulation overestimated the data by a factor of 5. At an energy deposit cut of 5 keV, the simulation agreed with the data.

We then extended our simulation to the situation of the G_E^n experiment and the “transversity” experiment. The rates are obtained with shielding protection as illustrated in Fig. 14. In the “transversity” experiment, the beam energy is 6.0 GeV; the beam current is $15 \mu\text{A}$ and the target is a 40 cm ^3He cell; the BigBite is at 30 degrees with 1.5 m drift. In the G_E^n experiment, the beam was 3.2 GeV at a current of $15 \mu\text{A}$ on a ^3He cell; the BigBite is at 54 degrees with 1.1 m drift distance. The rate results are listed in Table 11. The rates for the “transversity” experiment and the G_E^n experiment are similar, with an overall rate no more than 10-20 MHz per chamber.

Experiment	G_E^n Test run	Transversity	GEN
data	1.8 kHz/wire	(per chamber)	(per chamber)
simulation (5 keV cut)	$1.76 \pm 0.12 \pm 0.57$ kHz	7.5 ± 1.7 MHz	6.87 ± 1.62 MHz
simulation (1 keV cut)	$9.88 \pm 0.29 \pm 3.2$ kHz	20.2 ± 2.8 MHz	12.6 ± 2.2 MHz

Table 11: Wire chamber rate estimation for the G_E^n and the “transversity” experiment corresponding to 5 keV and 1 keV energy deposit cut in the simulation.

B Appendix-II. Separation of Collins and Sivers asymmetries

For the events within each kinematic bin, we need to find parameters a and b which maximize the likelihood function:

$$L = \frac{1}{N} \prod_i^N \frac{1}{V(\phi_h^i, \phi_S^i)} \left[1 + a \sin(\phi_h^i + \phi_S^i) + b \sin(\phi_h^i - \phi_S^i) \right]. \quad (27)$$

in which N is the number of event. The relative phase space volume $V(\phi_h^i, \phi_S^i)$ at bin (ϕ_h, ϕ_S) can be obtained from the target-spin-averaged counts normalized in a way such that $\sum_i 1/V(\phi_h^i, \phi_S^i) = N$. The best fit parameters a and b satisfy two linear equations [59]:

$$\begin{aligned} \frac{a}{N} \sum_i \frac{\sin^2(\phi_h^i + \phi_S^i)}{V(\phi_h^i, \phi_S^i)} + \frac{b}{N} \sum_i \frac{\sin(\phi_h^i + \phi_S^i) \sin(\phi_h^i - \phi_S^i)}{V(\phi_h^i, \phi_S^i)} &= \frac{1}{N} \sum_i \frac{\sin(\phi_h^i + \phi_S^i)}{V(\phi_h^i, \phi_S^i)}, \\ \frac{a}{N} \sum_i \frac{\sin(\phi_h^i + \phi_S^i) \sin(\phi_h^i - \phi_S^i)}{V(\phi_h^i, \phi_S^i)} + \frac{b}{N} \sum_i \frac{\sin^2(\phi_h^i - \phi_S^i)}{V(\phi_h^i, \phi_S^i)} &= \frac{1}{N} \sum_i \frac{\sin(\phi_h^i - \phi_S^i)}{V(\phi_h^i, \phi_S^i)}. \end{aligned} \quad (28)$$

The solutions are:

$$a = \frac{1}{\Delta} \left[\beta \cdot \frac{1}{N} \sum_i \frac{\sin(\phi_h^i + \phi_S^i)}{V(\phi_h^i, \phi_S^i)} - \gamma \cdot \frac{1}{N} \sum_i \frac{\sin(\phi_h^i - \phi_S^i)}{V(\phi_h^i, \phi_S^i)} \right], \quad (29)$$

$$b = \frac{1}{\Delta} \left[\alpha \cdot \frac{1}{N} \sum_i \frac{\sin(\phi_h^i - \phi_S^i)}{V(\phi_h^i, \phi_S^i)} - \gamma \cdot \frac{1}{N} \sum_i \frac{\sin(\phi_h^i + \phi_S^i)}{V(\phi_h^i, \phi_S^i)} \right], \quad (30)$$

in which

$$\alpha = \frac{1}{N} \sum_i \frac{\sin^2(\phi_h^i + \phi_S^i)}{V(\phi_h^i, \phi_S^i)}, \quad \beta = \frac{1}{N} \sum_i \frac{\sin^2(\phi_h^i - \phi_S^i)}{V(\phi_h^i, \phi_S^i)}, \quad (31)$$

$$\gamma = \frac{1}{N} \sum_i \frac{\sin(\phi_h^i + \phi_S^i) \sin(\phi_h^i - \phi_S^i)}{V(\phi_h^i, \phi_S^i)}, \quad \Delta = \alpha \cdot \beta - \gamma^2. \quad (32)$$

The one standard deviation [59] of parameter a and b are given by:

$$\sigma_a = \frac{1}{\sqrt{N}} \cdot \sqrt{\frac{\beta}{\Delta}}, \quad \sigma_b = \frac{1}{\sqrt{N}} \cdot \sqrt{\frac{\alpha}{\Delta}}. \quad (33)$$

References

- [1] J.P. Ralston and D.E. Soper, Nucl. Phys. **B152**, 109 (1979).
- [2] R.L. Jaffe and X. Ji, Phys. Rev. Lett. **67**, 552 (1991).
- [3] C. Bourrely, J. Soffer and O. V. Teryaev, Phys. Lett. **B420** (1998) 375, hep-ph/9710224.
- [4] J. Soffer, *Phys. Rev. Lett.* **74**, 1292 (1995).
- [5] J.C. Collins, Nucl. Phys. **B396**, 61 (1993).
- [6] T. Meng, J. Pan, Q. Xie and W. Zhu, Phys. Rev. D **40**, 769 (1989).
- [7] D.W. Sivers, Phys. Rev. D **41**, 83 (1990).
- [8] M. Anselmino, M. Boglione, and F. Murgia, Phys. Rev. D **60**, 054027 (1999).
- [9] S.J. Brodsky, D.S. Hwang, I. Schmidt, Phys. Lett. **B530**, 99 (2002).
- [10] M. Burkardt, Phys. Rev. D **69**, 057501 (2004)
- [11] D. Boer, P.J. Mulders, Phys. Rev. D **57**, 5780 (1998).
- [12] A. Airapetian *et al.* (HERMES), Phys. Rev. Lett. **94**, 012002 (2005), and M. Dieffenhaller *et al.*, hep-ex/0507013.
- [13] The COMPASS Collaboration, Phys. Rev. Lett. **94**, 202002 (2005).
- [14] A. Airapetian *et al.*, (HERMES), Phys. Rev. Lett. **84**, 4047 (2002); Phys. Rev. D **64**, 097101 (2001); Phys. Lett. **B562**, 182 (2003).
- [15] M. Boglione and P.J. Mulders, Phys. Lett. **B478**, 114 (2000).
- [16] M. Anselmino and F. Murgia, Phys. Lett. **B483**, 74 (2000).
- [17] A.V. Efremov, K. Goeke, and P. Schweitzer, Eur. Phys. J. **C24**, 407 (2002).
- [18] B.-Q. Ma, I. Schmidt and J.-J. Yang, Phys. Rev. D **66**, 094001 (2002).
- [19] A.V. Efremov, K. Goeke, and P. Schweitzer, Eur. Phys. J. **C32**, 337 (2003).
- [20] P. Schweitzer and A. Bacchetta, Nucl. Phys. **A732**, 106 (2004).
- [21] A. Bacchetta, A. Metz and J.-J. Yang, Phys. Lett. **B574**, 225 (2003).
- [22] L.P. Gamberg, G.R. Goldstein, and K.A. Oganessyan, Phys. Rev. D **68**, 051501 (2003).
- [23] S.J. Brodsky, D.S. Hwang, and I. Schmidt, Phys. Lett. **B530**, 99 (2002).
- [24] X. Ji, and F. Yuan, Phys. Lett. **B543**, 66 (2002).

- [25] J.C. Collins, Phys. Lett. **B536**, 43 (2002).
- [26] M. Anselmino, M. Boglione, U. D'Alesio, and F. Murgia, Phys. Rev. D **71**, 014002 (2005).
- [27] B.-Q. Ma, I. Schmidt, and J.-J Yang, Eur. Phys. J **C40**, 63 (2005).
- [28] R. Seidl (Belle Collaboration), to be published in the proceedings of SPIN 2004 (Trieste).
- [29] A. Bacchetta, hep-ph/0307282.
- [30] Alessandro Bacchetta, Umberto D'Alesio, Markus Diehl, C. Andy Miller, *Phys. Rev. D* **70**, 117504 (2004).
- [31] A. Airapetian *et al.* (HERMES), hep-ex/0505042.
- [32] M. Anselmino *et al.*, *et al.*, Phys. Rev. **D72**, 094007 (2005).
- [33] M. Anselmino *et al.*, hep-ph/0507181.
- [34] W. Vogelsang and F. Yuan, Phys. Rev. **D72**, 054028 (2005).
- [35] F. Yuan, private communication.
- [36] H. Avakian *et al.*, hep-ex/0301005.
- [37] JLab E02-013, Spokespersons: G. Cates, K. McCormick, B. Reitz and B. Wojtsekhowski.
- [38] P. Degtiarenko, private communications, 2005.
- [39] M. Iodice *et al.*, Performance and results of the RICH detector for kaon physics in Hall A at Jefferson Lab, Proceedings of RICH2004, to be published in Nucl. Instr. and Methods A.
- [40] JLab experiment E05-009, B. Wojtsekhowski, G. Cates, V. Nelyubin and P. E. Reimer co-spokespersons.
- [41] http://hallaweb.jlab.org/targets/polhe3/polhe3_tgt.html;
and tech notes in <http://www.jlab.org/e94010/>.
- [42] M. Amarian *et al.*, Phys. Rev. Lett. 89, 242301 (2002); 92, 022301 (2004); 93, 152301 (2004); Z. Meiziani, *et al.*, Phys. Lett. B 613, 148 (2005).
- [43] W. Xu, *et al.*, Phys. Rev. Lett. 85, 2900 (2000); F. Xiong, *et al.*, Phys. Rev. Lett. 87, 242501 (2001).
- [44] X. Zheng, *et al.*, Phys. Rev. Lett. 92, 012004 (2004); Phys. Rev. C 70, 065207 (2004).
- [45] K. Kramer, *et al.*, Phys. Rev. Lett. 95, 142002 (2005).

- [46] JLab E01-012, Spokespersons, J. P. Chen, S. Choi, N. Liyanage.
- [47] JLab E97-110, Spokespersons, J. P. Chen, A. Deur and F. Garibaldi.
- [48] E. Babcock, *et al.*, Phys. Rev. Lett. 91, 123003 (2003).
- [49] Lai, H.L. *et al.*, *Eur. Phys. J.* **C12**, 375 (2000).
- [50] B. A. Kniehl, G. Kramer, and B. Potter, *Nucl. Phys.* B **582**, 514 (2000).
- [51] P. Geiger, Ph.D. Dissertation, Ruprecht-Karls-University, Heidelberg (1998).
- [52] J.L. Friar *et al.*, Phys. Rev. C **42**, 2310 (1990).
- [53] A. Nogga, Ph. D. thesis, Ruhr-Universität Bochum, Bochum, Germany (2001), p.72.
- [54] C. Ciofi degli Atti *et al.*, Phys. Rev. C **48**, R968 (1993).
- [55] F. Bissey *et al.*, Phys. Rev. C **64**, 024004 (2001);
- [56] R. Ent,H. Mkrtchyan and P. Bosted, private communications.
- [57] A. Airapetian *et al.* (HERMES Collaboration), Phys. Rev. D **71**, 012003 (2005).
- [58] P. Lenisa, and F. Rathmann for the PAX Collaboration, hep-ex/0505054.
- [59] P. R. Bevington and D. K. Robinson, “ Data reduction and error analysis for the physical sciences”, The McGraw-Hill Companies Inc. 1992.